Higgs boson coupling measurements in ATLAS

LHCP 2024

Antonio Jesús Gómez Delegido (IFIC, CSIC-UV),
on behalf of the ATLAS collaboration

ATLAS EXPERIMENT

GOBIERNO DE ESPAÑA
MINISTERIO DE CIENCIA, INNOVACIÓN Y UNIVERSIDADES

Financiado por la Unión Europea NextGenerationEU
Plan de Recuperación, Transformación y Resiliencia
AGENCIA ESTATAL DE INVESTIGACIÓN

IFIC INSTITUT DE FÍSICA CORPUSCULAR
CSIC
VNIVERSITAT DE VALÈNCIA

Supported by AEI grant PID2021-124912NB-I00 and
FPU 2019 grant funded by
MCIN/AEI/10.13039/501100011033

Introduction

- After the discovery of the Higgs boson by ATLAS and CMS, the **measurement** of its **properties** has been a priority.
- Coupling between the Higgs boson and particles defined by the particle's mass and type. Three types of couplings to massive particles:

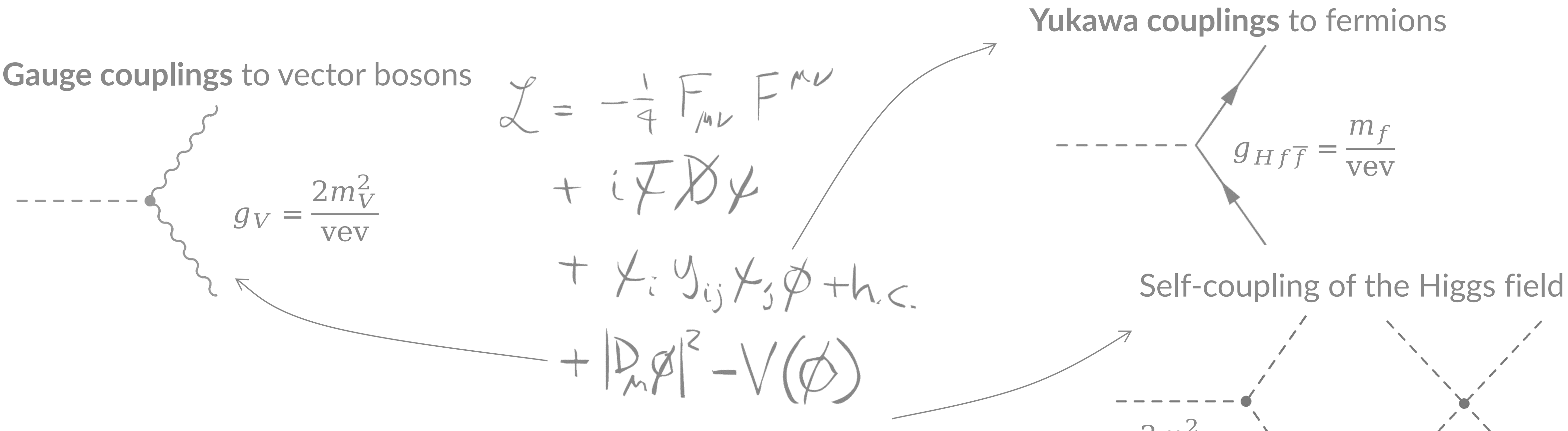

- Precision measurements of couplings are crucial:
  - Test of spontaneous symmetry-breaking mechanism (gauge couplings).
  - Test for Standard Model (SM) predictions in the Higgs sector (Yukawa interacions and self-interaction).

Higgs boson production and decay

- ATLAS recorded 140 fb^{-1} of pp collisions in Run 2 → According to SM prediction, ~9 millions of Higgs bosons, 0.3% experimentally accessible.

Production (13 TeV)

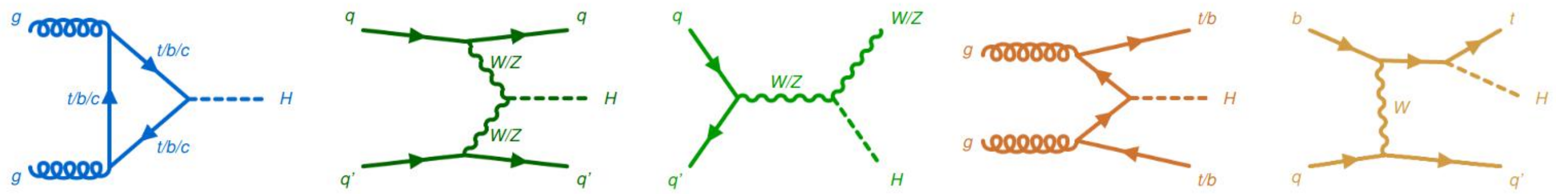

87% | 7% | 4% | 1% | <1%

Decay (m_H)

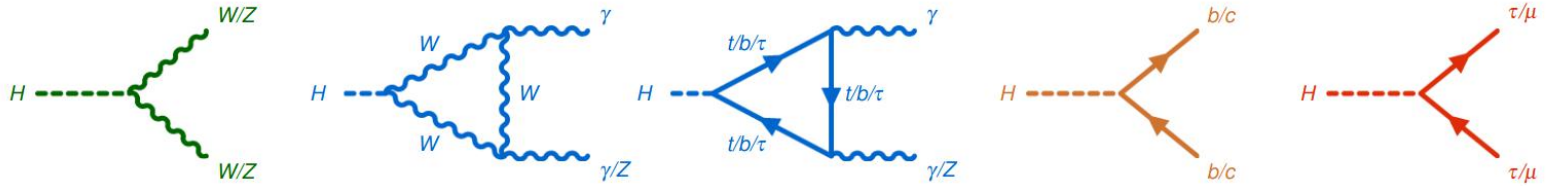

22% (WW)/3% (ZZ) | 0.2% ($\gamma\gamma$)/0.2% ($Z\gamma$) | 58% (bb)/2.9% (cc) | 6% ($\tau\tau$)/0.02% ($\mu\mu$)

- All **major** Higgs boson **production** and **decay** modes **observed** during Run 2. **Evidence** for **rare decays** (second generation couplings, $Z\gamma$) emerging.

- Experimentally well-established analyses used to probe **challenging phase spaces**.

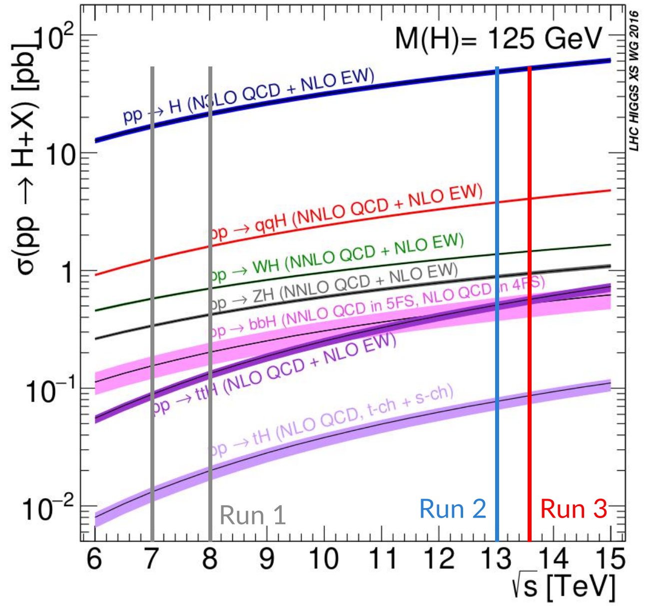

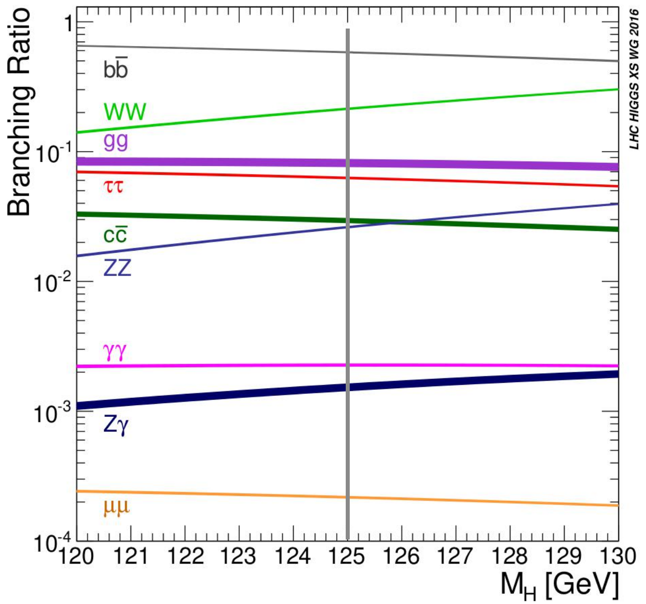

Combining Run 2 data

- **Combining** statistical power of **different decay signatures** → key to achieve sensitive cross-section/branching ratio measurements.
  - Fundamental to test precisely the SM.

- Global signal strength ($\mu = \sigma/\sigma_{SM}$):

$$\mu = 1.05 \pm 0.06 =$$
$$= 1.05 \pm 0.03 \pm 0.03 \pm 0.04 \pm 0.02$$

(stat.) (exp.) (sig. th.) (bkg. th.)

- **Different sensitivities** to the Higgs production modes **from different decay processes**. Excellent overall agreement with the SM.

Nature 607, pages 52-59 (2022)

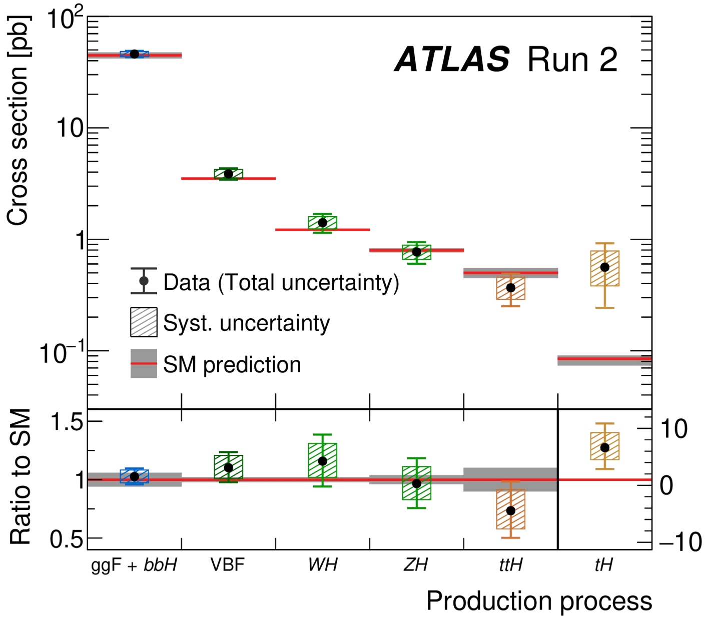

Nature 607, pages 52-59 (2022)

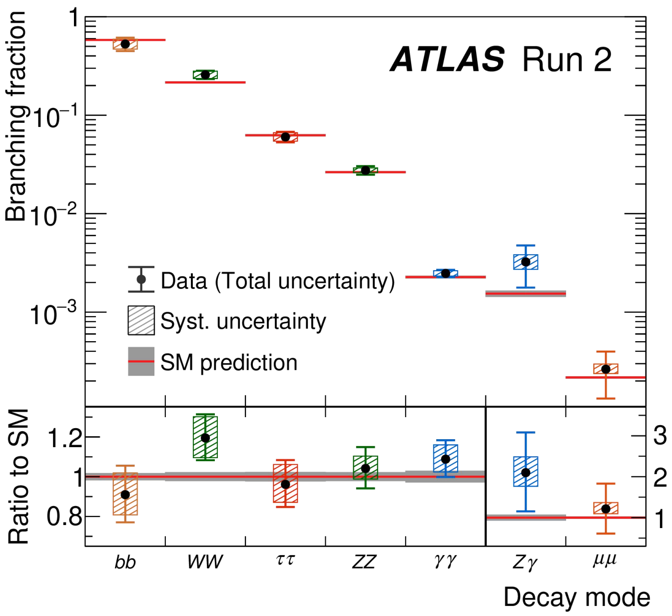

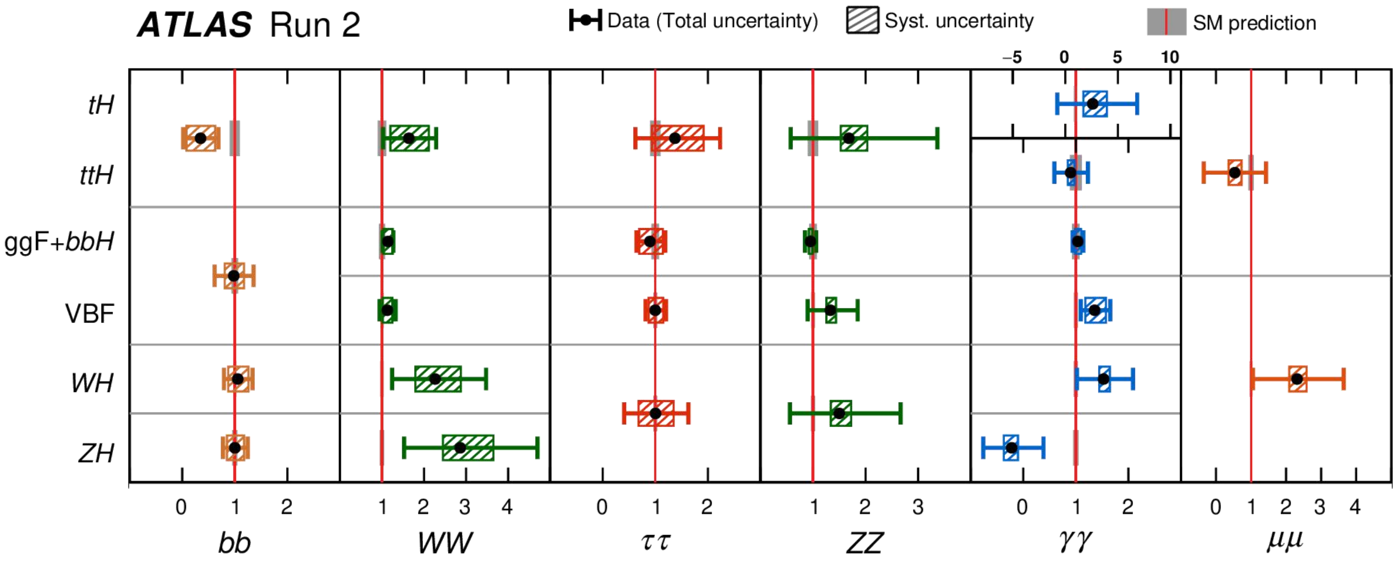

Nature 607, pages 52-59 (2022)

Combining Run 2 data - Coupling measurements

- Coupling fit performed within κ framework: κ modifiers affect coupling strength without altering kinematic distributions.

$$\sigma_i \times B(H \to f) = \frac{\kappa_i^2 \kappa_f^2}{\kappa_H^2} \sigma_i^{SM} \times B^{SM}(H \to f)$$

$$\kappa_i = \frac{\sigma_i}{\sigma_i^{SM}} \text{ or } \kappa_i = \frac{\Gamma_i}{\Gamma_i^{SM}}$$

$$\kappa_H^2 = \left(\frac{\Gamma_i}{\Gamma_i^{SM}}\right)^2 = \frac{\sum_p B_p^{SM} \kappa_p^2}{1 - B_{inv.} - B_{u.}}$$

- Different models tested with progressively fewer assumptions:

a) Modifiers for fermions (κ_F) and bosons (κ_V)

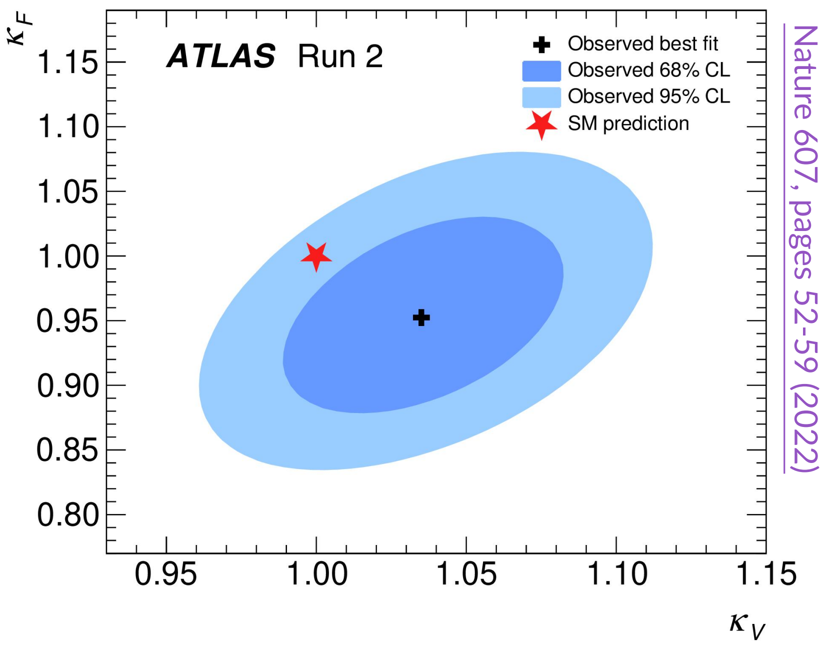

b) Independent couplings for W, Z, t, b, c, τ and μ

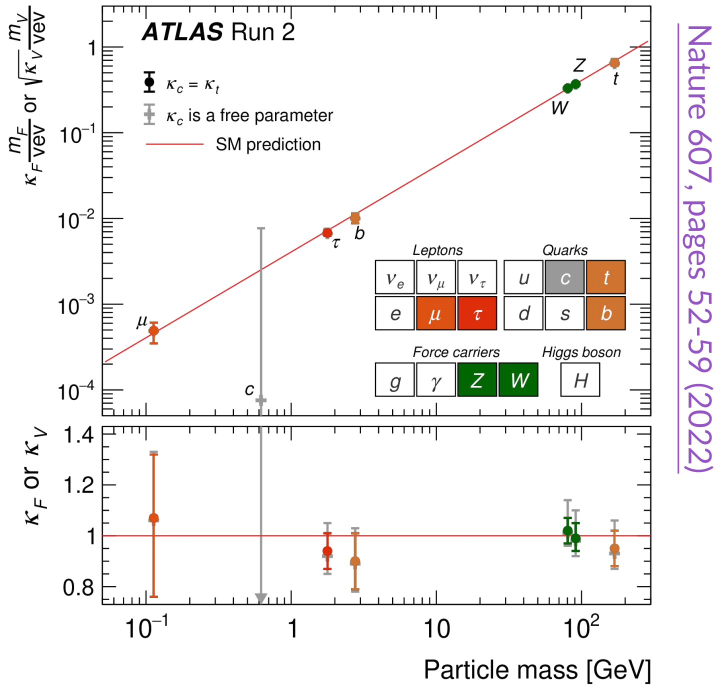

c) Include effective coupling strengths (κ_g, κ_γ, $\kappa_{Z\gamma}$)

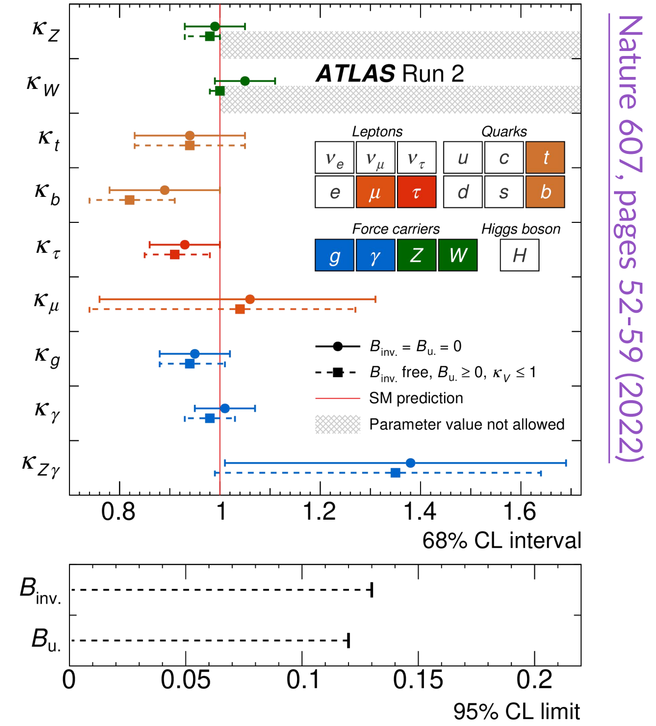

Combining Run 2 data - Simplified template cross-sections

- Simplified template cross-sections (STXS):
  - **Phase space partitioned** using **kinematic properties** of the Higgs boson (and associated objects like jets or vector bosons).
  - Designed to:
    - Optimize sensitivity to **BSM effects**.
    - Keep **theory uncertainties** under control.
    - Minimize model dependence.
- Simultaneous measurement of 36 phase space regions.
- Good agreement with the SM prediction, p-value of 94%.

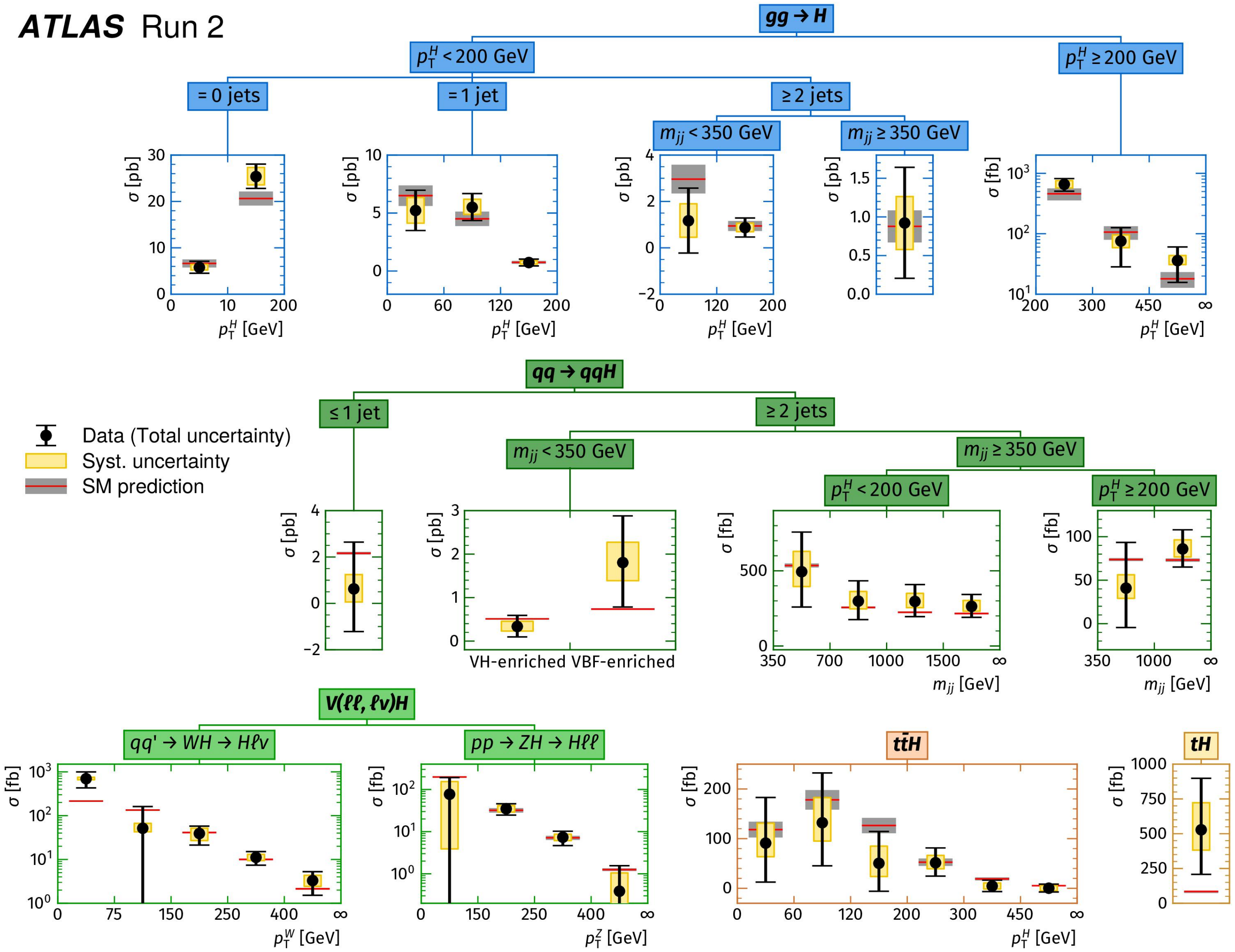

Nature 607, pages 52-59 (2022)

Interpretations in SMEFT

- Combined STXS results interpreted in **SM effective field theory**.
- Higher-dimensional operators built upon SM fields, scaled by Wilson-coefficients.

Wilson coefficient

$$\mathcal{L}_{\text{SMEFT}} = \mathcal{L}_{\text{SM}} + \sum_{i}^{N_{d=6}} \frac{c_i}{\Lambda^2} O_i^{(6)} + \sum_{j}^{N_{d=8}} \frac{b_j}{\Lambda^4} O_j^{(8)} + \ldots,$$

- Full set of Wilson coefficients of $d = 6$ operators cannot be constrained simultaneously:
  - Large number of degrees of freedom.
  - Degeneracies in the impact of operators.
- **Principal component analysis** performed to choose **rotated basis**.

arXiv:2402.05742

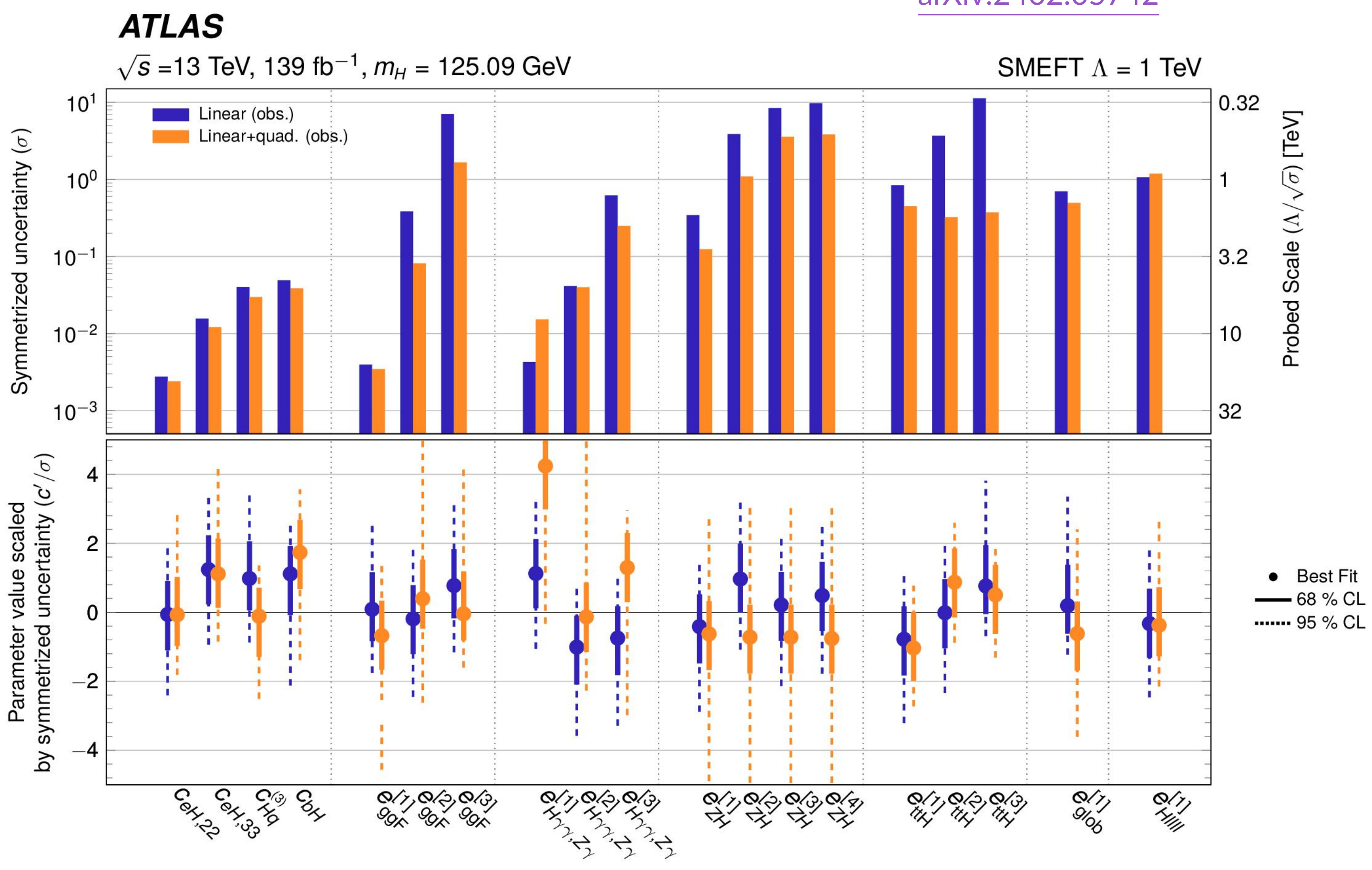

Linear term: interference between $d = 6$ operators and SM.
Quadratic term: Pure BSM, product of two $d = 6$ operators.

Relative sign of the W and Z couplings with VBF WH production

- **VBF $\boldsymbol{WH}$ production** provides unique **sensitivity to $\boldsymbol{\lambda_{WZ} = \kappa_W / \kappa_Z}$**. Destructive interference predicted by the SM. Enhanced production for $\lambda_{WZ} < 0$. Combinations have measured $|\lambda_{WZ}|$.
- Two separate analyses targeting VBF $WH \rightarrow jj\ell\nu b\bar{b}$, either BSM ($\lambda_{WZ} < 0$) or SM signal with dedicated regions to normalize main backgrounds ($t\bar{t}$, tW and W+jets).
- Results compatible with SM and background-only hypothesis. **Non-SM allowed region excluded with $> \boldsymbol{5\sigma}$**.
- Observed (expected) upper limit on VBF WH cross-section: 9.0 (8.7) SM prediction at 95% CL.

arXiv:2402.00426

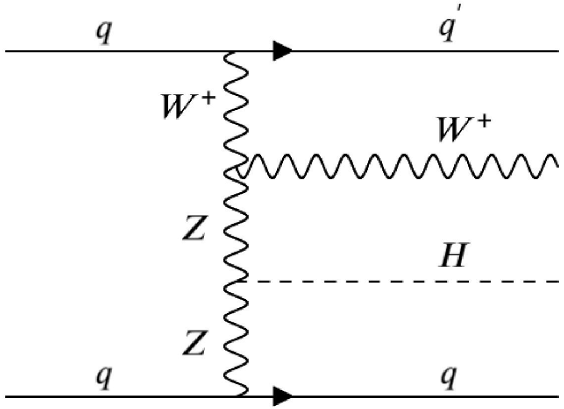

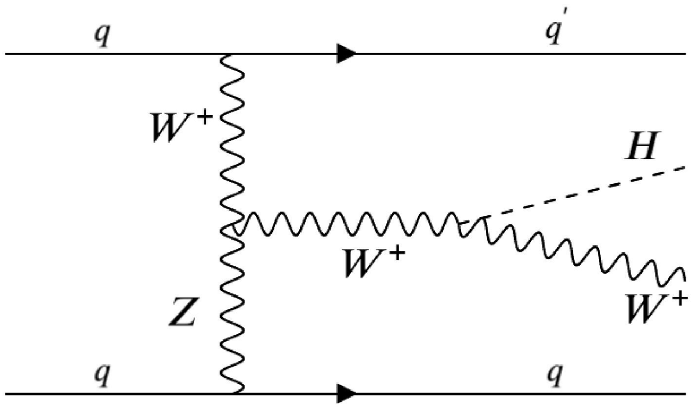

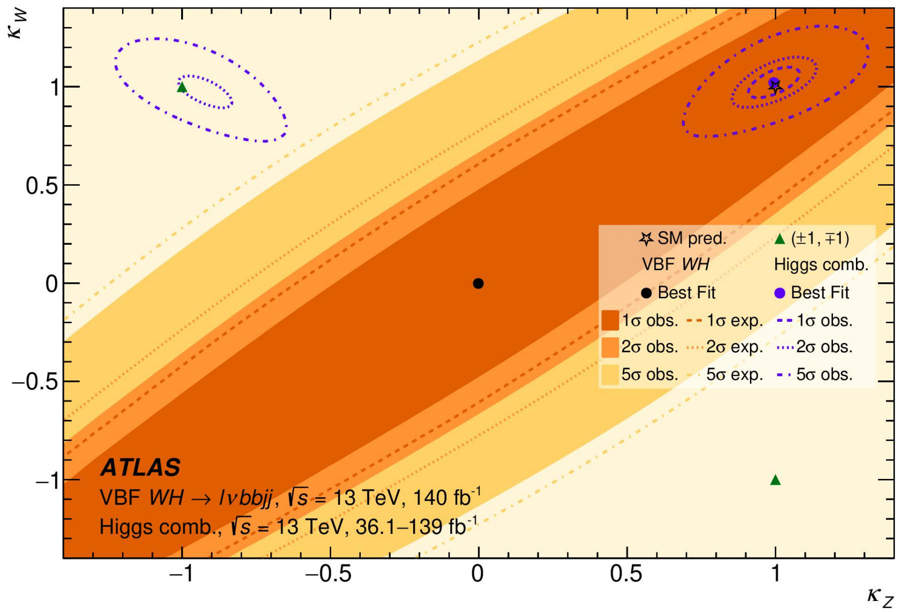

Boosted VH production in fully hadronic $qqbb$ final states

- First measurement of **boosted** (high p_{T}) Higgs production with $VH \rightarrow qqbb$. Sensitivity to **BSM effects**.
- Requiring **2 large-$\boldsymbol{R}$ jets** in signal enriched region: one passing $\boldsymbol{H \rightarrow bb}$ **tagging**, other **W/Z tagging**.
- Data driven estimation of major (>90%) multijet background and Z+jets normalization.
- Production **cross section** measured **inclusively** and in $\boldsymbol{p_{\mathrm{T}}^{H}}$ **ranges** using the Higgs candidate mass.

$$\mu_{\mathrm{inc}} = 1.4^{+1.0}_{-0.9}$$ 1.7σ obs. (1.2σ exp)

Phys. Rev. Lett. 132 (2024) 131802

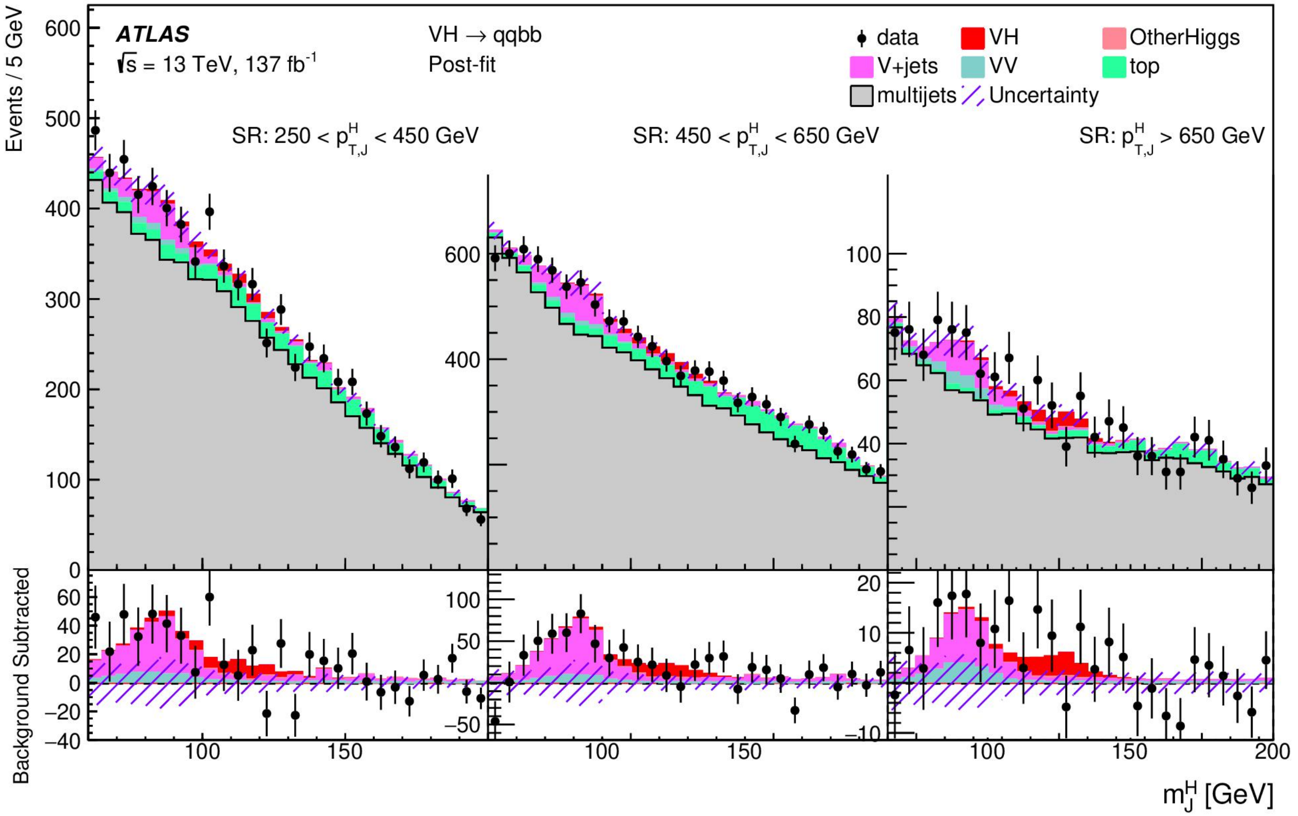

Kinematic region	Observed μ	Observed σ [fb]	Expected σ [fb]
$250 \leq p_{\mathrm{T}}^{H} < 450$ GeV, $\lvert y_H \rvert < 2$	$0.8^{+2.2}_{-1.9}$	47^{+125}_{-109}	57.0
$450 \leq p_{\mathrm{T}}^{H} < 650$ GeV, $\lvert y_H \rvert < 2$	$0.4^{+1.7}_{-1.5}$	2^{+10}_{-9}	5.9
$p_{\mathrm{T}}^{H} \geq 650$ GeV, $\lvert y_H \rvert < 2$	$5.3^{+11.3}_{-3.2}$	6^{+13}_{-4} (<43)	1.2

STXS measurements in $H \rightarrow \tau\tau$

NEW!

- New results expanding previous **STXS $H \rightarrow \tau\tau$ measurements** (JHEP 08 (2022) 175) in **VBF and $t\bar{t}H$ phase space**, keeping previous strategy for ggH (Boost) and VH.
- Events selected with **two τ candidates**. Three channels depending on **τ decay mode**: $\tau_{\rm had}\tau_{\rm had}$, $\tau_{\rm lep}\tau_{\rm had}$, $\tau_e\tau_\mu$.
- Additional selections to split events in ggH, VBF, VH and $t\bar{t}H$ categories. Further selections to target STXS regions.

ATLAS-CONF-2024-007

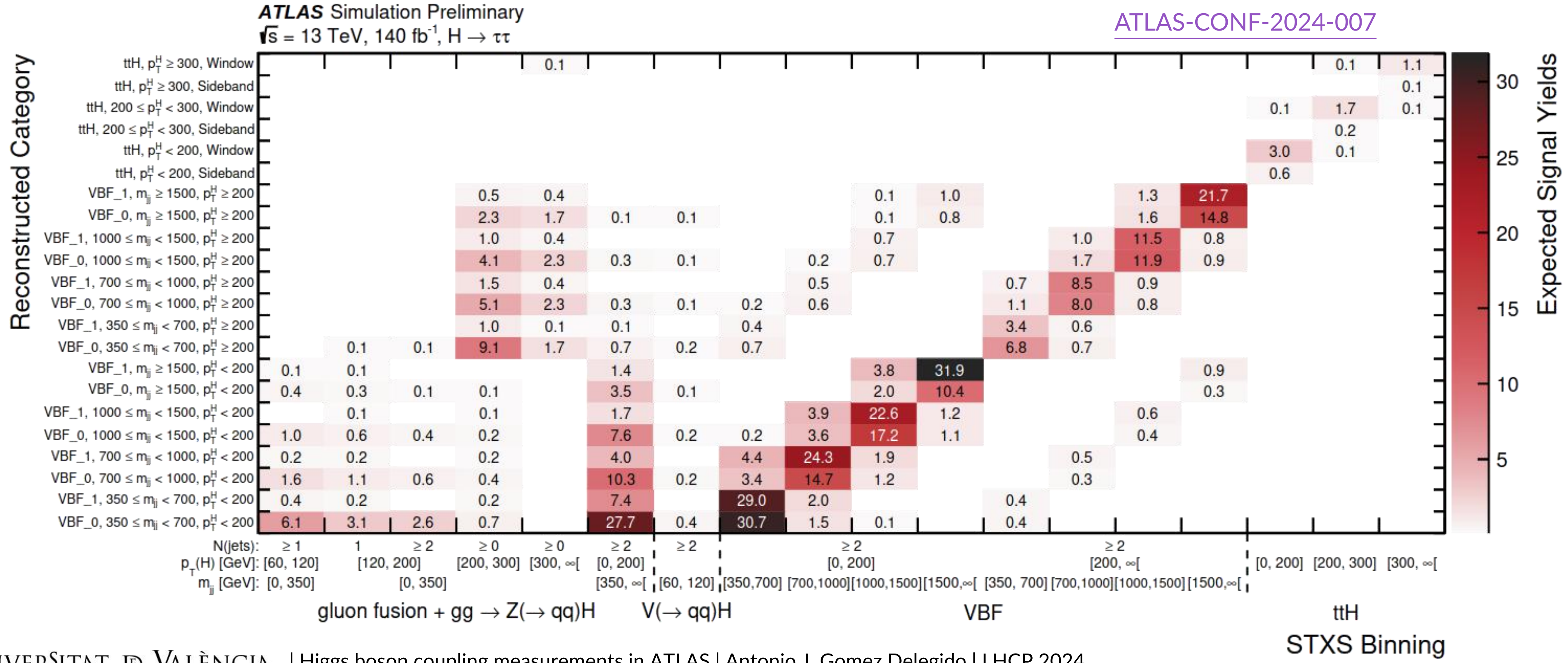

STXS measurements in $H \to \tau\tau$

ATLAS-CONF-2024-007

- Mass reconstructed using **Missing Mass Calculator** (Nucl. Instrum. Meth. **A 654** (2011) 481).
- $\boldsymbol{p_{\mathrm{T}}^{H}}$ **reconstruction** using novel **NN** exploiting $E_{\mathrm{T}}^{\mathrm{miss}}$ and $\tau\tau$ variables.
- **VBF BDT** using information from jets, τ and $E_{\mathrm{T}}^{\mathrm{miss}}$. Enhance separation betwen **VBF and ggH/$\boldsymbol{Z \to \tau\tau}$.**
- **Multiclass BDT** used in $t\bar{t}H$ to separate $\boldsymbol{t\bar{t}H}$ **from** $\boldsymbol{t\bar{t}}$ **and** $\boldsymbol{Z \to \tau\tau}$.

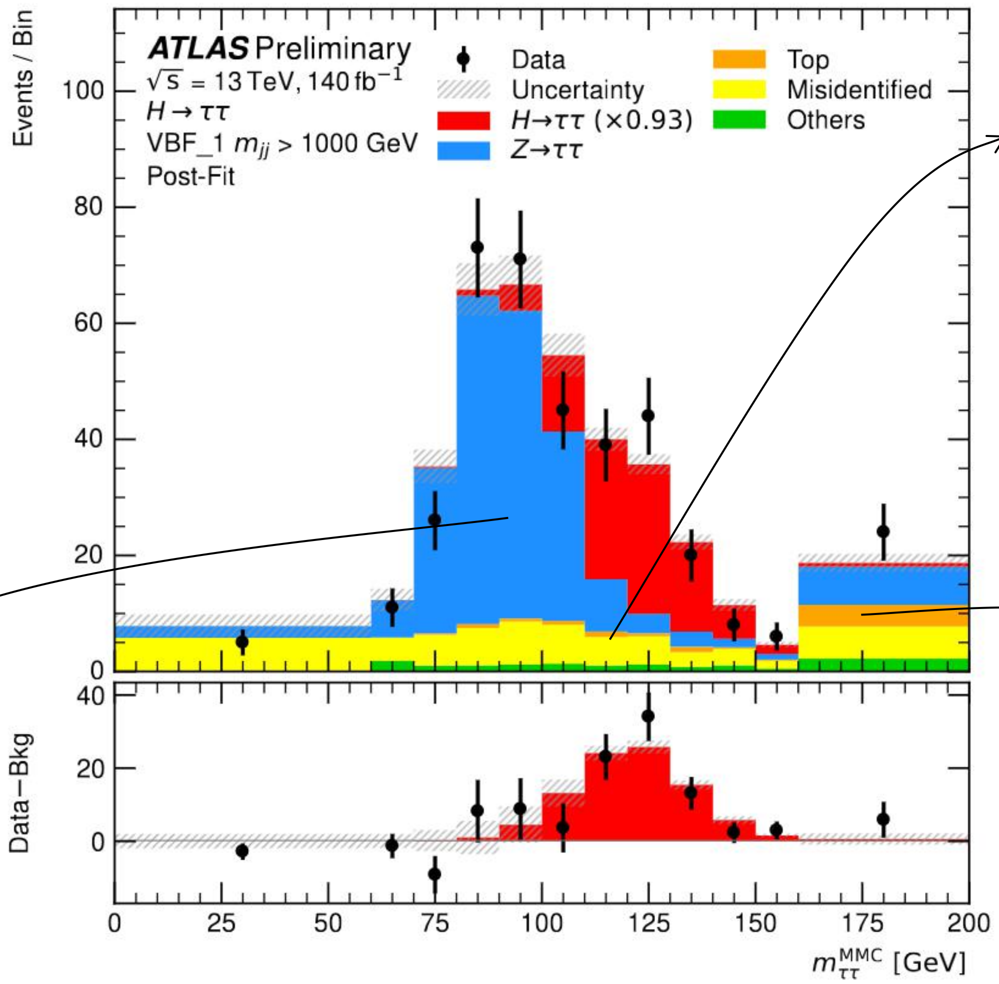

$Z \to \tau\tau$
- Main background.
- Modelled by MC simulation ($Z \to \tau\tau$ template shape).
- $Z \to \ell\ell$ modified through τ embedding used to extract normalization.

Misidentified objets
- Data-driven estimations computing transfer factors in regions enhanced in misidentified backgrounds.

Top and other backgrounds
- Estimated with MC.
- Top normalization extracted from data.

STXS measurements in $H \to \tau\tau$

- Fits across different regions with different free floating parameters:
  - 1 Parameter-of-interest (POI) fit to extract **overall signal strength with respect to SM.**
  - 4 POI fit to measure **different production** processes separately. Good agreement wih SM, p-value of 99%.
    - VBF production
      - Slightly better precision with respect to last publication due to improved categorization.
    - $t\bar{t}H$ production
      - Refined multivariate analysis approach leads to **~25% improvement**.

ATLAS-CONF-2024-007

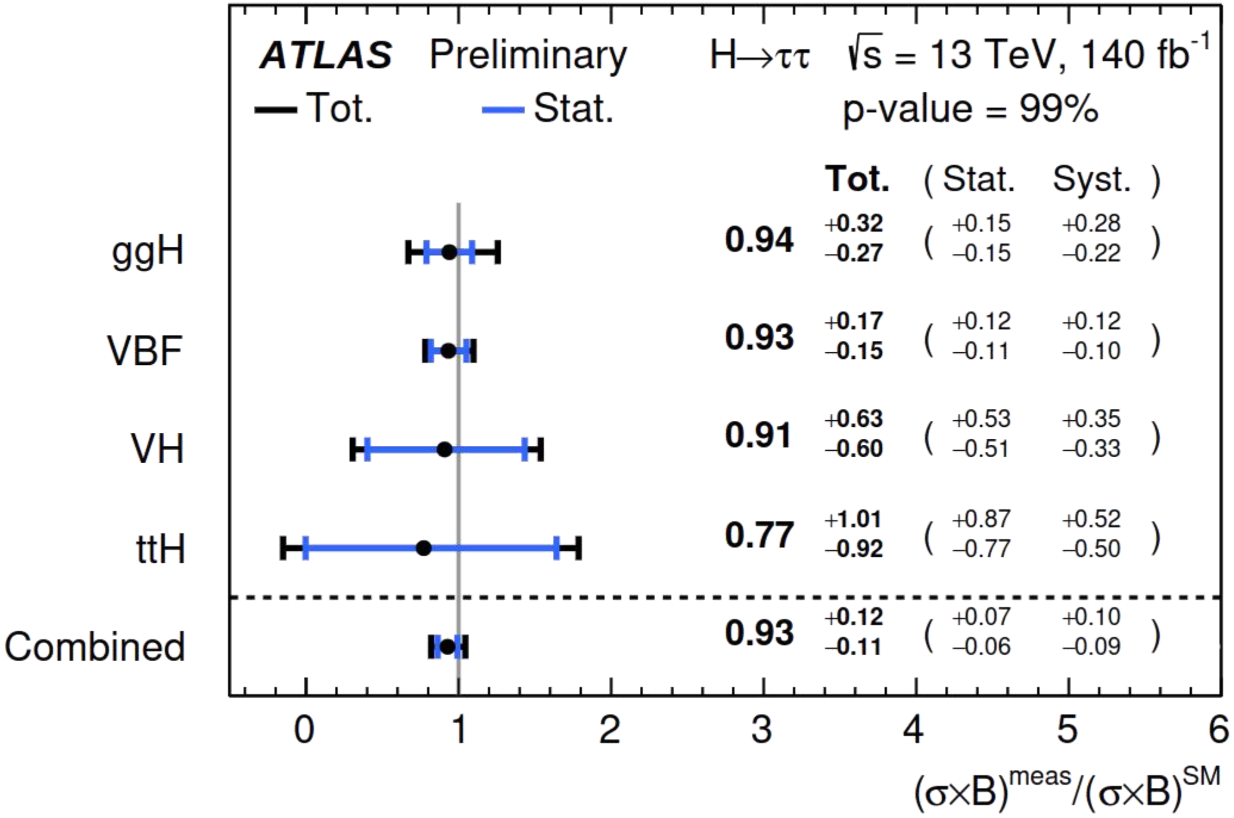

STXS measurements in $H \to \tau\tau$

ATLAS-CONF-2024-007

- Fits across different regions with different free floating parameters:
  - 18 POI fit corresponding to different STXS regions.
    - Better **precision** in VBF phase space for **higher p_T^H and/or m_{jj}** due to **reduced SM backgrounds**.
    - Reasonable agreement with SM prediction with p-value of 6%.
    - **$t\bar{t}H$ results statistically limited**. Upper limits at 95% CL derived for $t\bar{t}H$ in STXS framework.

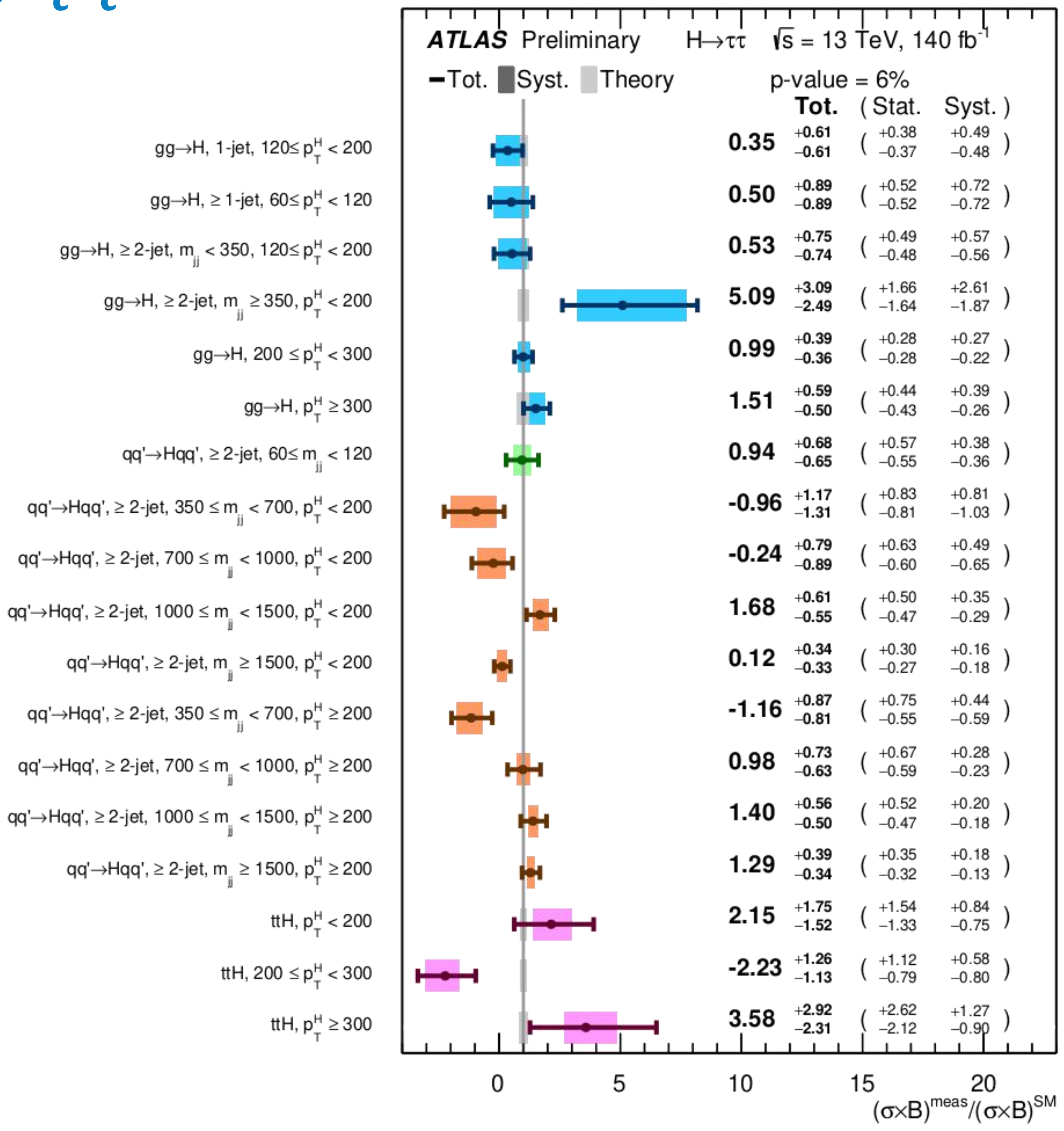

STXS measurements in $H \rightarrow \tau\tau$

- Fits across different regions with different free floating parameters:
  - 18 POI fit corresponding to different STXS regions.
    - Better **precision** in VBF phase space for **higher p_T^H and/or m_{jj}** due to **reduced SM backgrounds**.
    - Reasonable agreement with SM prediction with p-value of 6%.
    - **$t\bar{t}H$ results statistically limited**. Upper limits at 95% CL derived for $t\bar{t}H$ in STXS framework.

ATLAS-CONF-2024-007

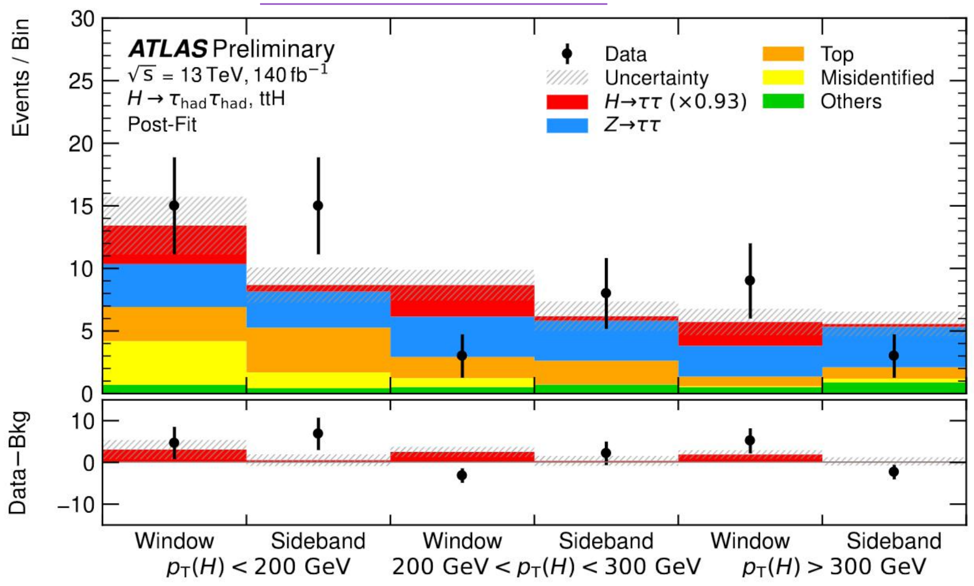

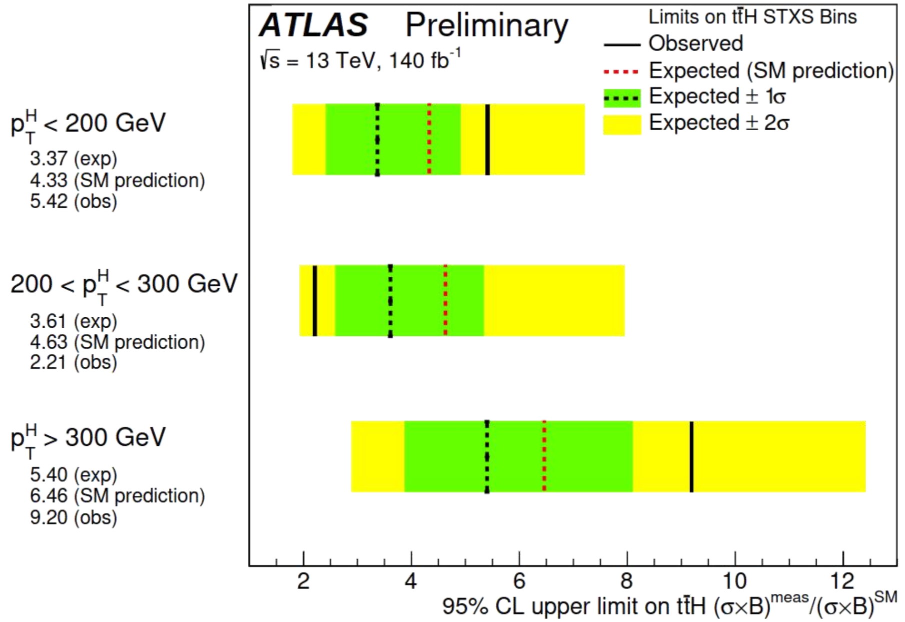

ATLAS-CONF-2024-007

Searches for rare Higgs boson decays

- Probing the coupling of the Higgs boson to second-generation fermions:
  - $\boldsymbol{H \to \mu\mu}$
    - Large **Drell-Yan background**. Events sorted targeting different production modes. Fit to $m_{\mu\mu}$.
    - Observed (expected) significance over background-only hypothesis is $\boldsymbol{2.0\sigma}$ (1.7σ) for $m_H = 125.09$ GeV.
  - $\boldsymbol{H \to cc}$
    - $VH,\ H \to cc$. Challenging search, where **c-tagging efficiency** (27%) is crucial. Simultaneous fit on m_{cc} in various categories.
    - Observed (expected) **upper limit** on signal strength of **26 (31) times the SM** prediction at 95% CL.

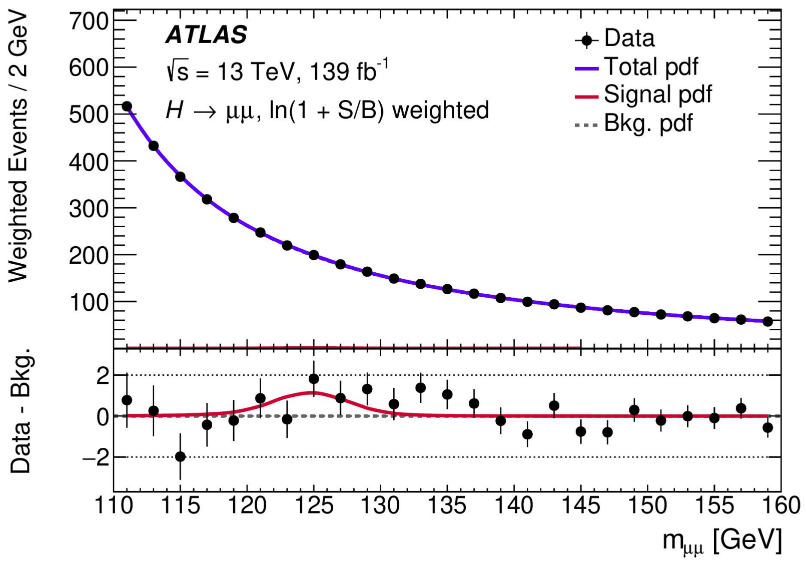

Phys. Lett. B 812 (2021) 135980

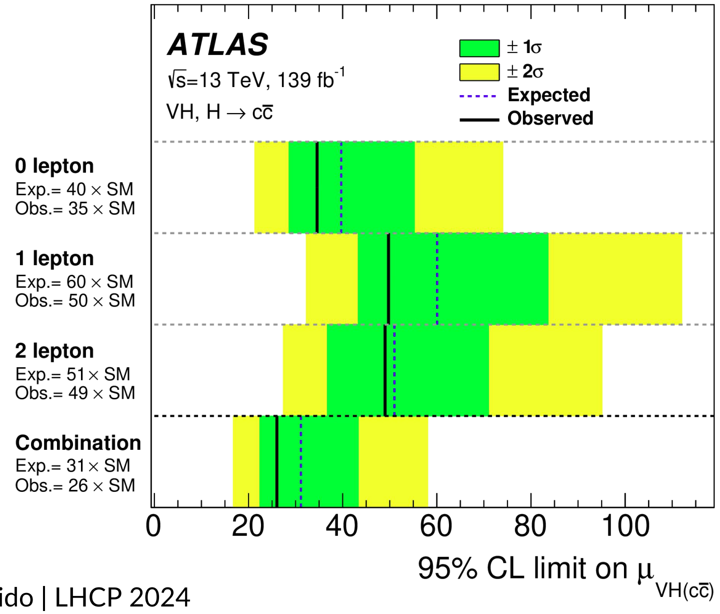

Eur. Phys. J. C 82 (2022) 717

Conclusions

Nature 607, pages 52-59 (2022)

- Presented a selection of ATLAS results. Very good agreement with SM.
- **Precision era**. Coupling measurements with uncertainties $< 10\%$.
- Main couplings exploited to explore **extreme and challenging phase space regions**.
- Continuous effort to measure **rare decays** and extend coupling measurements to second-generation fermions.

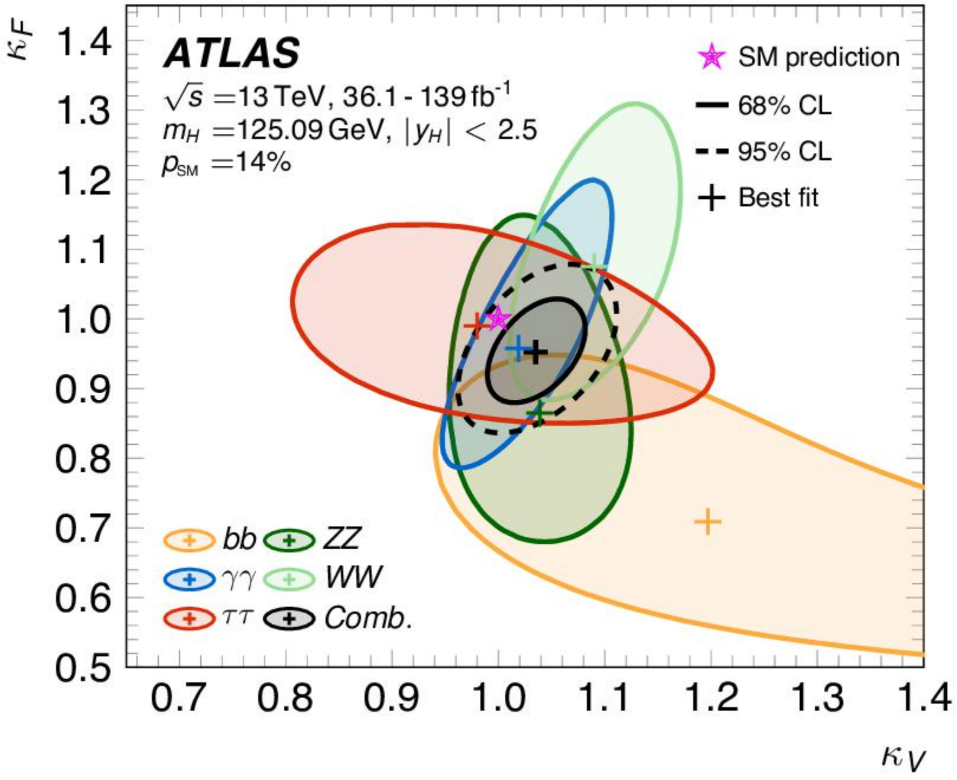

Additional material

Coupling modifiers and STXS measurements

	(a) $B_{inv.} = B_{u.} = 0$	(b) $B_{inv.}$ free, $B_{u.} \geq 0$, $\kappa_{W,Z} \leq 1$
κ_Z	$0.99^{+0.06}_{-0.06}$	$0.98^{+0.02}_{-0.05}$
κ_W	$1.05^{+0.06}_{-0.06}$	$1.00_{-0.02}$
κ_t	$0.94^{+0.11}_{-0.11}$	$0.94^{+0.11}_{-0.11}$
κ_b	$0.89^{+0.11}_{-0.11}$	$0.82^{+0.09}_{-0.08}$
κ_τ	$0.93^{+0.07}_{-0.07}$	$0.91^{+0.07}_{-0.06}$
κ_μ	$1.06^{+0.25}_{-0.30}$	$1.04^{+0.23}_{-0.30}$
κ_g	$0.95^{+0.07}_{-0.07}$	$0.94^{+0.07}_{-0.06}$
κ_γ	$1.01^{+0.06}_{-0.06}$	$0.98^{+0.05}_{-0.05}$
$\kappa_{Z\gamma}$	$1.38^{+0.31}_{-0.37}$	$1.35^{+0.29}_{-0.36}$
$B_{inv.}$	-	< 0.13
$B_{u.}$	-	< 0.12

Nature 607, pages 52-59 (2022)

STXS	Cross section [pb]	SM prediction [pb]
$gg \to H$, 0-jet, $p_T^H < 10$ GeV	$5.8 \pm 1.3(^{+1.2}_{-1.1}(stat.)^{+0.7}_{-0.6}(syst.))$	6.6 ± 0.9
$gg \to H$, 0-jet, $10 \leq p_T^H < 200$ GeV	$25.4^{+2.7}_{-2.6}(\pm 1.8(stat.)^{+2.0}_{-1.8}(syst.))$	20.6 ± 1.5
$gg \to H$, 1-jet, $p_T^H < 60$ GeV	$5.2 \pm 1.7(\pm 1.3(stat.) \pm 1.1(syst.))$	6.5 ± 0.9
$gg \to H$, 1-jet, $60 \leq p_T^H < 120$ GeV	$5.5^{+1.2}_{-1.1}(\pm 1.0(stat.)^{+0.7}_{-0.6}(syst.))$	4.5 ± 0.6
$gg \to H$, 1-jet, $120 \leq p_T^H < 200$ GeV	$0.73^{+0.30}_{-0.29}(\pm 0.25(stat.)^{+0.16}_{-0.14}(syst.))$	0.75 ± 0.13
$gg \to H$, ≥ 2-jet, $m_{jj} < 350$ GeV, $p_T^H < 120$ GeV	$1.2 \pm 1.4(\pm 1.2(stat.) \pm 0.7(syst.))$	3.0 ± 0.6
$gg \to H$, ≥ 2-jet, $m_{jj} < 350$ GeV, $120 \leq p_T^H < 200$ GeV	$0.9 \pm 0.4(\pm 0.4(stat.) \pm 0.2(syst.))$	0.94 ± 0.22
$gg \to H$, ≥ 2-jet, $m_{jj} \geq 350$ GeV, $p_T^H < 200$ GeV	$0.9 \pm 0.7(\pm 0.6(stat.) \pm 0.3(syst.))$	0.88 ± 0.21
$gg \to H$, $200 \leq p_T^H < 300$ GeV	$0.66^{+0.16}_{-0.15}(^{+0.13}_{-0.12}(stat.)^{+0.10}_{-0.08}(syst.))$	0.46 ± 0.10
$gg \to H$, $300 \leq p_T^H < 450$ GeV	$0.08 \pm 0.05(^{+0.05}_{-0.04}(stat.) \pm 0.02(syst.))$	0.106 ± 0.027
$gg \to H$, $p_T^H \geq 450$ GeV	$0.036^{+0.024}_{-0.020}(^{+0.023}_{-0.020}(stat.)^{+0.008}_{-0.005}(syst.))$	0.018 ± 0.005
$qq \to Hqq$, ≤ 1-jet	$0.6^{+2.0}_{-1.8}(^{+1.9}_{-1.8}(stat.) \pm 0.6(syst.))$	2.16 ± 0.06
$qq \to Hqq$, ≥ 2-jet, $m_{jj} < 350$ GeV, VH-enriched	$0.34^{+0.26}_{-0.24}(^{+0.23}_{-0.22}(stat.)^{+0.12}_{-0.11}(syst.))$	0.510 ± 0.016
$qq \to Hqq$, ≥ 2-jet, $m_{jj} < 350$ GeV, VBF-enriched	$1.8^{+1.1}_{-1.0}(^{+1.0}_{-0.9}(stat.)^{+0.5}_{-0.4}(syst.))$	0.735 ± 0.019
$qq \to Hqq$, ≥ 2-jet, $350 \leq m_{jj} < 700$ GeV, $p_T^H < 200$ GeV	$0.49^{+0.26}_{-0.24}(^{+0.23}_{-0.21}(stat.)^{+0.13}_{-0.10}(syst.))$	0.535 ± 0.013
$qq \to Hqq$, ≥ 2-jet, $700 \leq m_{jj} < 1000$ GeV, $p_T^H < 200$ GeV	$0.30^{+0.14}_{-0.12}(^{+0.12}_{-0.11}(stat.)^{+0.06}_{-0.05}(syst.))$	0.256 ± 0.007
$qq \to Hqq$, ≥ 2-jet, $1000 \leq m_{jj} < 1500$ GeV, $p_T^H < 200$ GeV	$0.30^{+0.11}_{-0.10}(^{+0.10}_{-0.09}(stat.)^{+0.05}_{-0.04}(syst.))$	0.224 ± 0.006
$qq \to Hqq$, ≥ 2-jet, $m_{jj} \geq 1500$ GeV, $p_T^H < 200$ GeV	$0.26^{+0.08}_{-0.07}(\pm 0.07(stat.)^{+0.04}_{-0.03}(syst.))$	0.216 ± 0.006
$qq \to Hqq$, ≥ 2-jet, $350 \leq m_{jj} < 1000$ GeV, $p_T^H \geq 200$ GeV	$0.04 \pm 0.05(^{+0.05}_{-0.04}(stat.)^{+0.02}_{-0.01}(syst.))$	0.0737 ± 0.0017
$qq \to Hqq$, ≥ 2-jet, $m_{jj} \geq 1000$ GeV, $p_T^H \geq 200$ GeV	$0.086^{+0.022}_{-0.021}(\pm 0.019(stat.)^{+0.011}_{-0.009}(syst.))$	0.0732 ± 0.0019
$qq \to Hl\nu$, $p_T^V < 75$ GeV	$0.70^{+0.30}_{-0.27}(^{+0.29}_{-0.26}(stat.)^{+0.06}_{-0.04}(syst.))$	0.215 ± 0.008
$qq \to Hl\nu$, $75 \leq p_T^V < 150$ GeV	$0.05^{+0.11}_{-0.08}(^{+0.11}_{-0.08}(stat.)^{+0.02}_{-0.01}(syst.))$	0.134 ± 0.005
$qq \to Hl\nu$, $150 \leq p_T^V < 250$ GeV	$0.039^{+0.019}_{-0.018}(\pm 0.013(stat.)^{+0.013}_{-0.012}(syst.))$	0.0412 ± 0.0017
$qq \to Hl\nu$, $250 \leq p_T^V < 400$ GeV	$0.011 \pm 0.004(^{+0.004}_{-0.003}(stat.) \pm 0.002(syst.))$	0.0100 ± 0.0004
$qq \to Hl\nu$, $p_T^V \geq 400$ GeV	$0.0033^{+0.0020}_{-0.0018}(^{+0.0017}_{-0.0016}(stat.)^{+0.0011}_{-0.0009}(syst.))$	0.00214 ± 0.00011
$gg/qq \to Hll$, $p_T^V < 150$ GeV	$0.08 \pm 0.11(^{+0.09}_{-0.08}(stat.)^{+0.08}_{-0.07}(syst.))$	0.198 ± 0.007
$gg/qq \to Hll$, $150 \leq p_T^V < 250$ GeV	$0.035^{+0.011}_{-0.010}(^{+0.009}_{-0.008}(stat.)^{+0.007}_{-0.006}(syst.))$	0.032 ± 0.004
$gg/qq \to Hll$, $250 \leq p_T^V < 400$ GeV	$0.0074^{+0.0029}_{-0.0027}(^{+0.0025}_{-0.0024}(stat.)^{+0.0013}_{-0.0012}(syst.))$	0.0072 ± 0.0008
$gg/qq \to Hll$, $p_T^V \geq 400$ GeV	$0.0004^{+0.0012}_{-0.0011}(^{+0.0010}_{-0.0009}(stat.)^{+0.0007}_{-0.0006}(syst.))$	0.00126 ± 0.00010
$t\bar{t}H$, $p_T^H < 60$ GeV	$0.09^{+0.09}_{-0.08}(^{+0.08}_{-0.07}(stat.)^{+0.04}_{-0.03}(syst.))$	0.118 ± 0.016
$t\bar{t}H$, $60 \leq p_T^H < 120$ GeV	$0.13^{+0.10}_{-0.09}(^{+0.09}_{-0.08}(stat.)^{+0.05}_{-0.04}(syst.))$	0.178 ± 0.020
$t\bar{t}H$, $120 \leq p_T^H < 200$ GeV	$0.05 \pm 0.06(\pm 0.05(stat.) \pm 0.03(syst.))$	0.126 ± 0.015
$t\bar{t}H$, $200 \leq p_T^H < 300$ GeV	$0.052^{+0.030}_{-0.027}(^{+0.026}_{-0.024}(stat.)^{+0.015}_{-0.012}(syst.))$	0.053 ± 0.007
$t\bar{t}H$, $300 \leq p_T^H < 450$ GeV	$0.005^{+0.012}_{-0.011}(\pm 0.010(stat.) \pm 0.006(syst.))$	0.0190 ± 0.0031
$t\bar{t}H$, $p_T^H \geq 450$ GeV	$0.000 \pm 0.008(^{+0.006}_{-0.005}(stat.) \pm 0.005(syst.))$	0.0054 ± 0.0010
tH	$0.5^{+0.4}_{-0.3}(\pm 0.3(stat.)^{+0.2}_{-0.1}(syst.))$	$0.085^{+0.005}_{-0.011}$

Nature 607, pages 52-59 (2022)

STXS measurements

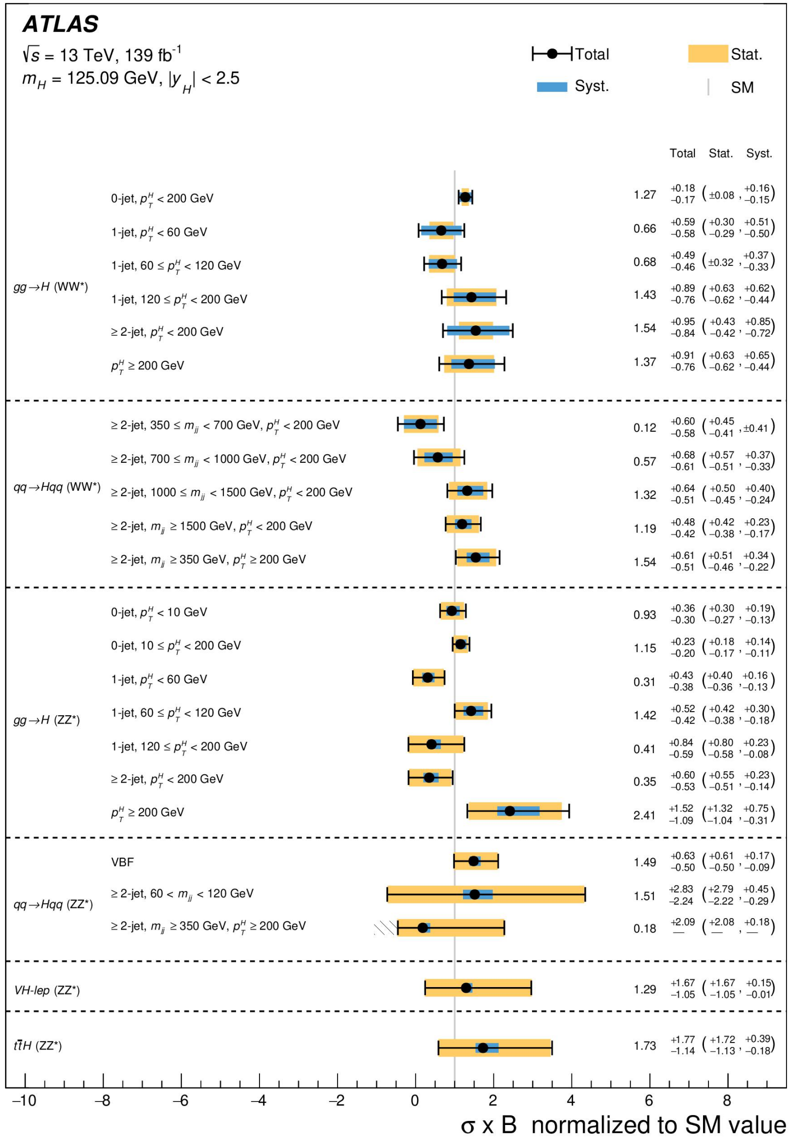

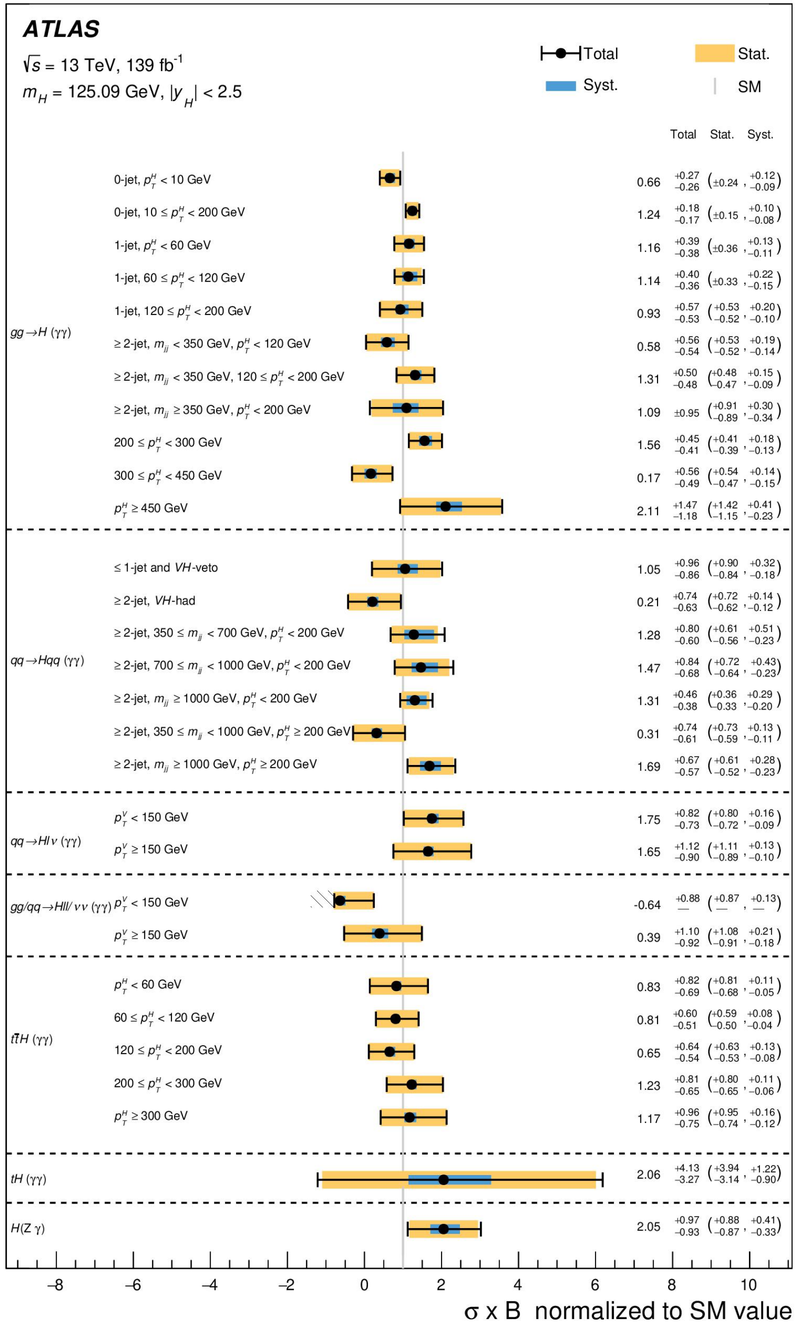

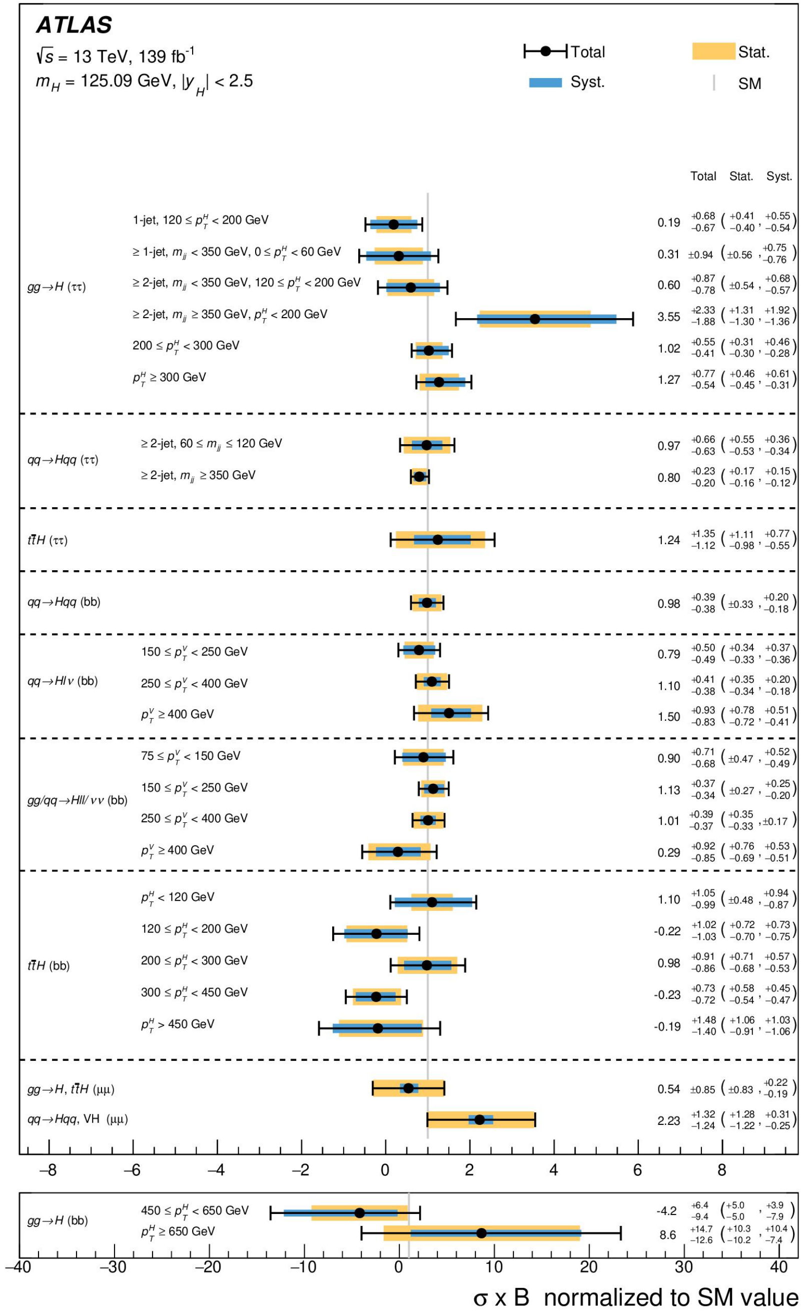

Interpretations in SMEFT

arXiv:2402.05742

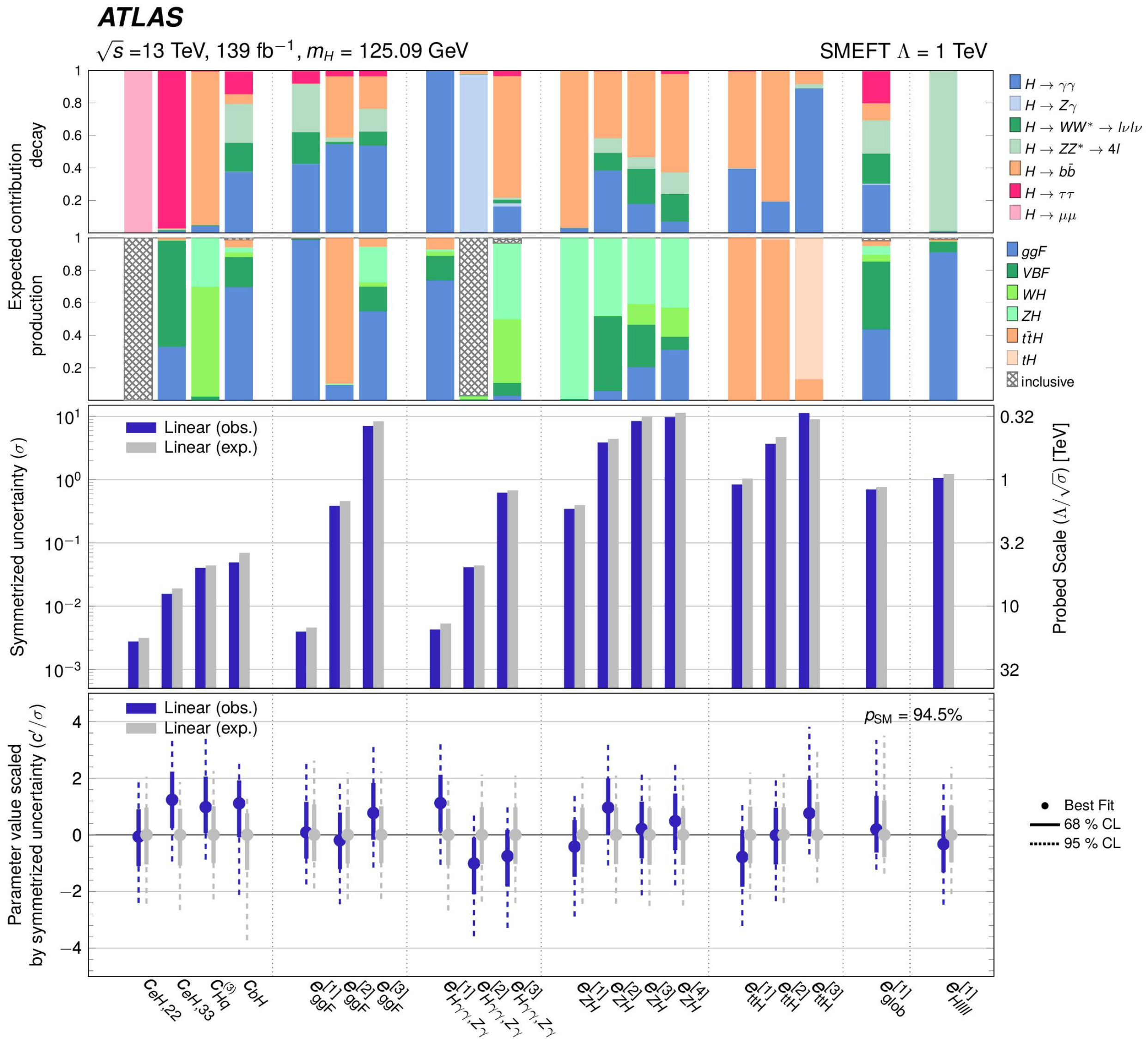

Interpretations in SMEFT

arXiv:2402.05742

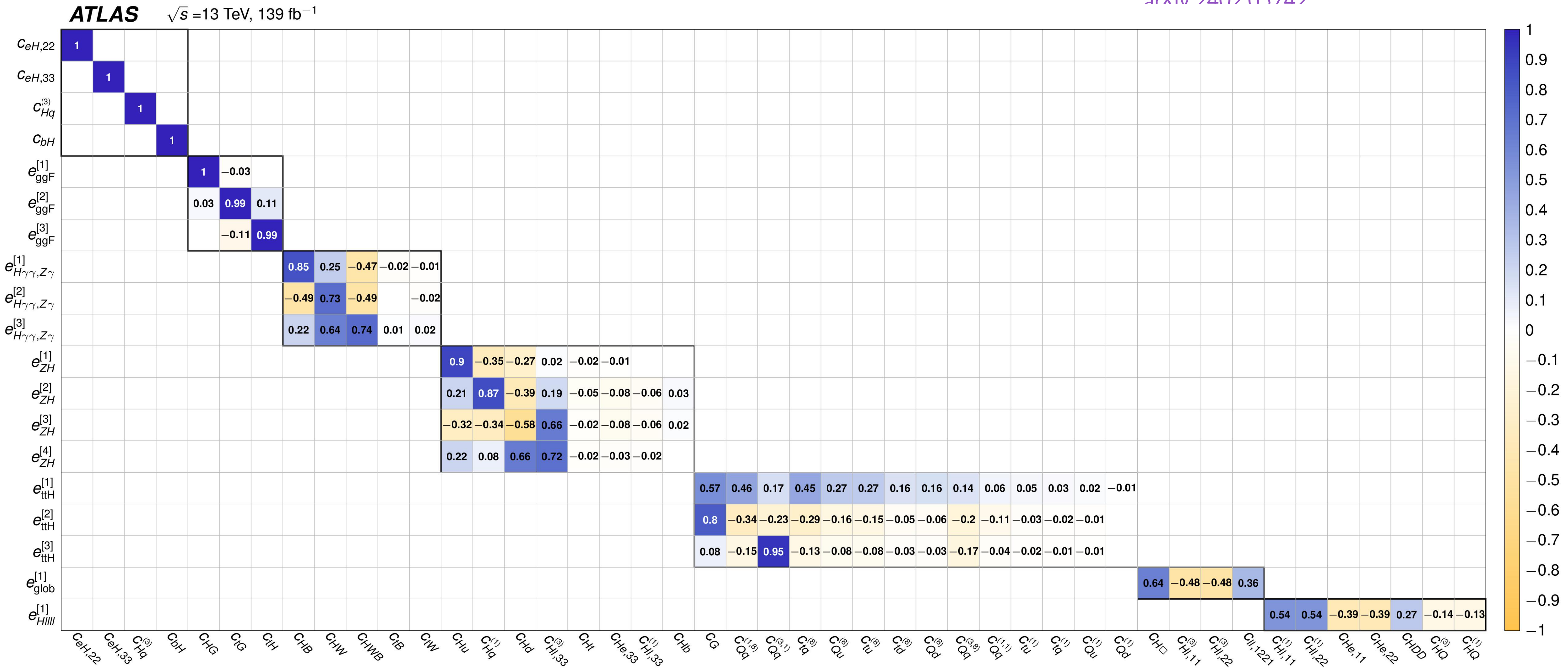

Relative sign of the W and Z couplings with VBF WH production

arXiv:2402.00426

Variable	Description	SR^-	SR^+_{loose}	SR^+_{tight}
$m_{b\bar{b}}$	Invariant mass of the two b-jets ($b\bar{b}$ system).	$\in$ (105, 145) GeV	$\in$ (105, 145) GeV	$\in$ (105, 145) GeV
$\Delta R_{b\bar{b}}$	ΔR between the two b-jets.	< 1.2	< 1.6	< 1.2
$p_T^{b\bar{b}}$	p_T of the $b\bar{b}$ system.	> 250 GeV	> 100 GeV	> 180 GeV
m_{jj}	Invariant mass of the VBF jets.	–	> 600 GeV	> 1000 GeV
Δy_{jj}	Rapidity separation of the VBF jets.	> 4.4	> 3.0	> 3.0
m_{top}^{lep}	Invariant mass of the W and either b-jet that is closest to 172.7 GeV.	> 260 GeV	> 260 GeV	> 260 GeV
$\xi_{Wb\bar{b}}$	$\frac{\lvert y_{Wb\bar{b}} - y_{jj}\rvert}{\Delta y_{jj}}$, where $y_{Wb\bar{b}}$ (y_{jj}) is the rapidity of the $Wb\bar{b}$ (VBF-jet) system.	< 0.3	< 0.3	< 0.3
$\Delta\phi(Wb\bar{b}, jj)$	Azimuthal separation between the $Wb\bar{b}$ system and the VBF-jet system.	–	–	> 2.7
N_{jets}^{veto}	Number of nontagged, non-VBF jets with p_T > 25 GeV and $\lvert\eta\rvert$ < 2.5.	–	≤ 1	= 0

arXiv:2402.00426

	Negative λ_{WZ}	Positive λ_{WZ}
$k_{t\bar{t}}$	$0.88^{+0.30}_{-0.35}$	$0.96^{+0.21}_{-0.23}$
k_W	$1.12^{+0.34}_{-0.25}$	$1.25^{+0.33}_{-0.24}$
k_{Wt}	$0.32^{+0.39}_{-0.13}$	$0.31^{+0.37}_{-0.14}$
$\mu = \sigma/\sigma_{pred.}$	$-0.027^{+0.054}_{-0.057}$	$0.9^{+4.0}_{-4.3}$

	SR^-	SR^+_{loose}	SR^+_{tight}
$t\bar{t}$	42 ± 19	172 ± 35	15.0 ± 5.8
W+jets	26 ± 13	84 ± 32	14.1 ± 7.6
Wt	4.6 ± 7.0	8 ± 13	0.8 ± 1.5
Other background	5.4 ± 1.6	16.2 ± 4.2	3.0 ± 1.5
Total background	77.7 ± 8.6	279 ± 15	32.9 ± 5.8
VBF WH, pre-fit	285 ± 45	4.15 ± 0.56	2.30 ± 0.62
VBF WH, post-fit	−8 ± 17	4 ± 17	2.2 ± 9.8
Data	70	274	37

Relative sign of the W and Z couplings with VBF WH production

Negative λ_{WZ}

Uncertainty source	$\Delta\mu$
$t\bar{t}$ modelling	± 0.033
Jet energy resolution	± 0.017
Wt modelling	± 0.013
Jet energy scale	± 0.011
Signal modelling	± 0.007
W+jets modelling	± 0.006
MC statistical uncertainty	± 0.005
Jet vertex tagging	± 0.003
Flavor tagging	± 0.002
E_T^{miss} scale and trigger efficiency	± 0.001
Luminosity and pileup reweighting	± 0.001
Other background modelling	± 0.001
Lepton scale and efficiency	< 0.001
Total systematic	± 0.045
Normalization factors	± 0.016
Total statistical	± 0.032
Total uncertainty	± 0.055

Positive λ_{WZ}

Uncertainty source	$\Delta\mu$
W+jets modelling	± 1.9
$t\bar{t}$ modelling	± 1.8
Jet energy resolution	± 1.3
Jet energy scale	± 0.8
MC statistical uncertainty	± 0.8
Other background modelling	± 0.5
Signal modelling	± 0.4
Wt modelling	± 0.3
E_T^{miss} scale and trigger efficiency	± 0.3
Flavor tagging	± 0.1
Luminosity and pileup reweighting	± 0.1
Jet vertex tagging	± 0.1
Lepton scale and efficiency	< 0.1
Total systematic	± 3.3
Normalization factors	± 1.4
Total statistical	± 2.5
Total uncertainty	± 4.1

arXiv:2402.00426

Boosted VH production in fully hadronic $qqbb$ final states

Uncertainty source	$\delta\mu$
Signal modeling	$^{+0.10}_{-0.02}$
MC statistical uncertainty	$^{+0.13}_{-0.13}$
Instrumental (pileup, luminosity)	$^{+0.012}_{-0.004}$
Large-R jet	$^{+0.13}_{-0.14}$
Top-quark modeling	$^{+0.14}_{-0.15}$
Other theory modeling	$^{+0.05}_{-0.03}$
$H \rightarrow b\bar{b}$ tagging	$^{+0.52}_{-0.23}$
Multijet estimate (TF uncertainty)	$^{+0.52}_{-0.41}$
Multijet modeling (TF vs. BDT)	$^{+0.14}_{-0.18}$
Total systematic uncertainty	$^{+0.80}_{-0.61}$
Signal statistical uncertainty	$^{+0.60}_{-0.60}$
Z+jets normalization	$^{+0.42}_{-0.20}$
Total statistical uncertainty	$^{+0.63}_{-0.63}$
Total uncertainty	$^{+1.02}_{-0.88}$

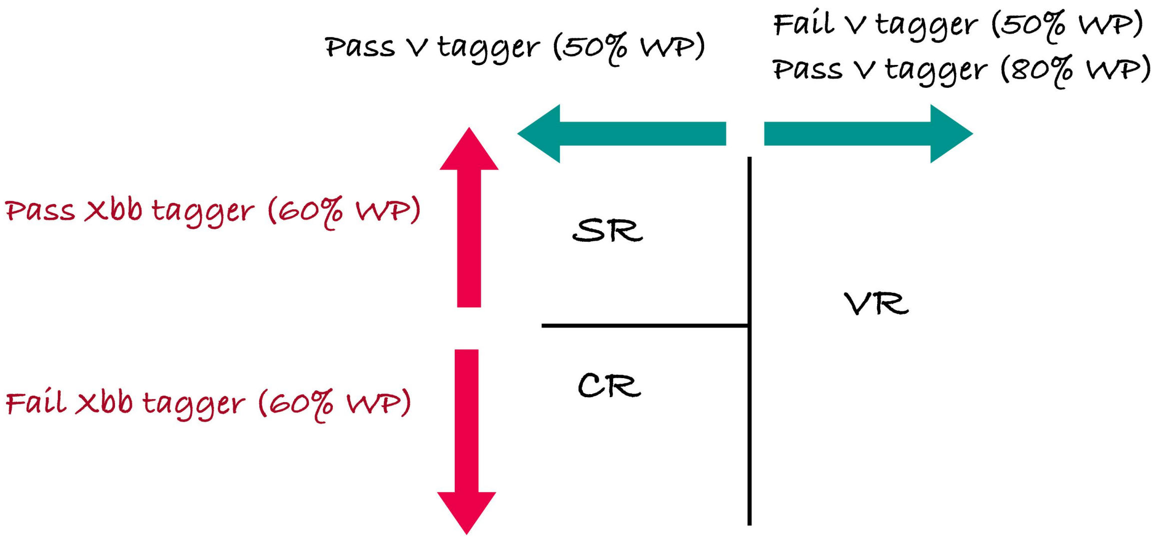

Phys. Rev. Lett. 132 (2024) 131802

Cross-section at 13.6 TeV with $H \to ZZ$ and $H \to \gamma\gamma$

- Inclusive Higgs boson production measured in $\gamma\gamma$ and $ZZ^* \to 4\ell$ channels using 31.4 fb^{-1} and 29 fb^{-1} of data from Run 3 pp collisions.
- Fiducial cross-sections measurements extracted via fit to recontructed invariant mass spectra.
- Individual measurements are extrapolated to full phase space and combined. First ATLAS Higgs production cross section measurement in Run 3, compatible with SM prediction of 59.9 ± 2.6 pb.

$$\sigma(pp \to H) = 58.2 \pm 7.5\ (\text{stat.})\ \pm 4.2\ (\text{syst.})\ \text{pb}$$

Eur. Phys. J. C 84 (2024) 78

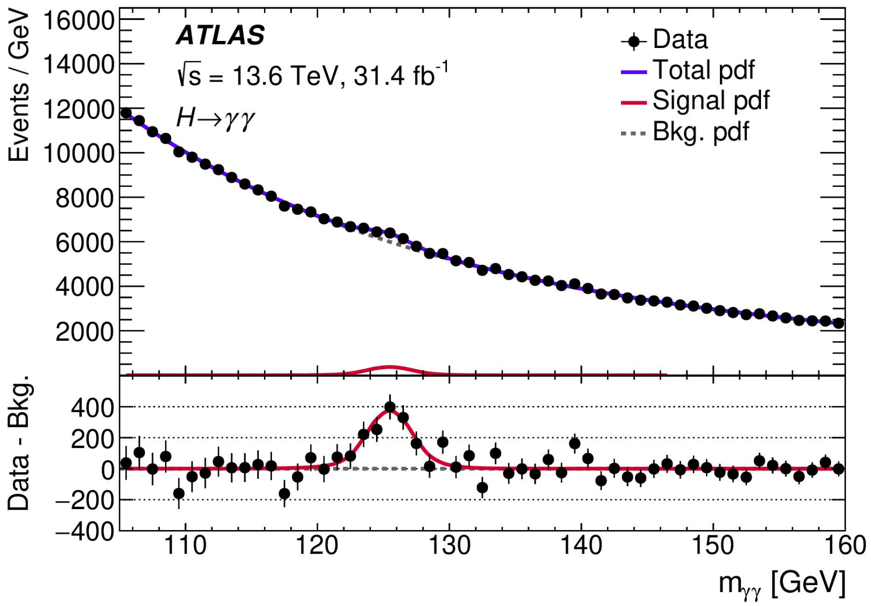

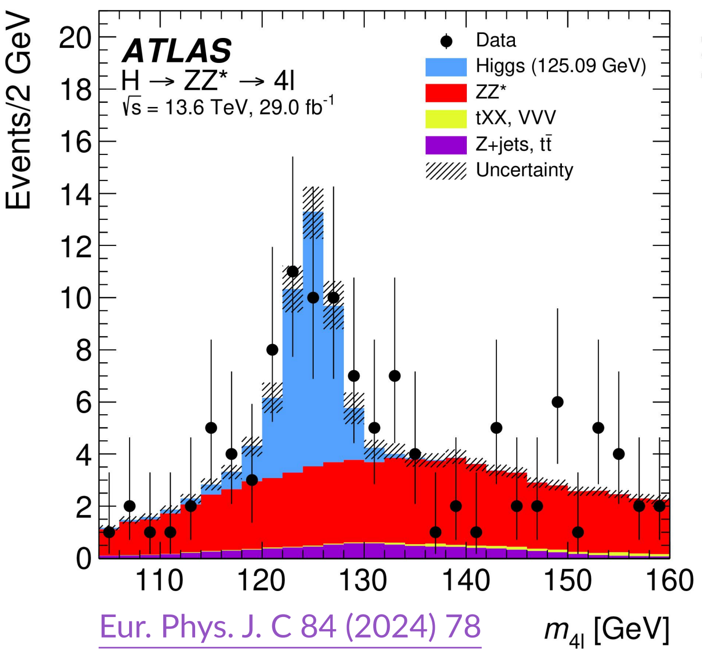

Eur. Phys. J. C 84 (2024) 78

Eur. Phys. J. C 84 (2024) 78

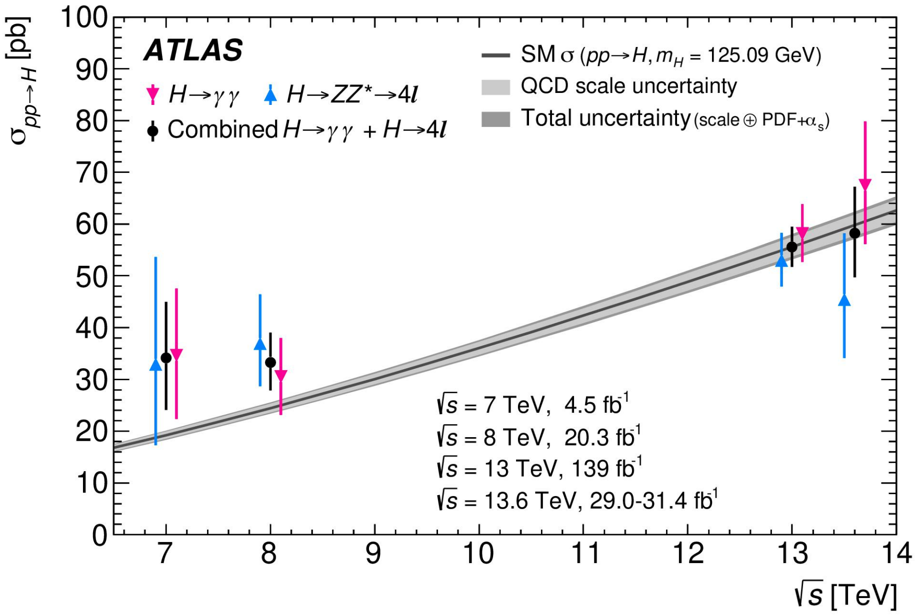

STXS measurements in $H \to \tau\tau$

	$\tau_e\tau_\mu$	$\tau_{\text{lep}}\tau_{\text{had}}$		$\tau_{\text{had}}\tau_{\text{had}}$
		$e\tau_{\text{had}}$	$\mu\tau_{\text{had}}$	
Preselection Object counting	# of $e = 1$, # of $\mu = 1$, # of $\tau_{\text{had-vis}} = 0$	# of $e/\mu = 1$, # of $\tau_{\text{had-vis}} = 1$		# of $e/\mu = 0$, # of $\tau_{\text{had-vis}} = 2$
p_{T} cut	e/μ : p_{T} cut 10 GeV to 27.3 GeV	e/μ : p_{T} cut 21 GeV to 27.3 GeV, $\tau_{\text{had-vis}}$: $p_{\text{T}} > 30$ GeV		$\tau_{\text{had-vis}}$: $p_{\text{T}} > 40$,30 GeV
ID, Isolation, and e-veto	e/μ: Medium e: Loose, μ: Tight	e/μ: Medium, $\tau_{\text{had-vis}}$: Medium e: Loose, μ: Tight 1-prong $\tau_{\text{had-vis}}$: eleBDT e-veto		$\tau_{\text{had-vis}}$: Medium
Charge product	Opposite charge	Opposite charge		Opposite charge
Kinematics	$m^{\text{coll}}_{\tau\tau} > m_Z - 25$ GeV $30 < m_{e\mu} < 100$ GeV	$m_{\text{T}} < 70$ GeV		
b-veto	# of b-jets $= 0$ DL1r 85% WP	# of b-jets $= 0$ DL1r 85% WP		# of b-jets $= 0$ DL1r 70% WP not applied in tt(0L)$H \to \tau_{\text{had}}\tau_{\text{had}}$
$E^{\text{miss}}_{\text{T}}$	$E^{\text{miss}}_{\text{T}} > 20$ GeV	$E^{\text{miss}}_{\text{T}} > 20$ GeV		$E^{\text{miss}}_{\text{T}} > 20$ GeV
Leading jet	$p_{\text{T}} > 40$ GeV	$p_{\text{T}} > 40$ GeV		$p_{\text{T}} > 70$ GeV, $\lvert\eta\rvert < 3.2$
Angular	$\Delta R_{e\mu} < 2.0$, $\lvert\Delta\eta_{e\mu}\rvert < 1.5$	$\Delta R_{\ell\tau_{\text{had-vis}}} < 2.5$, $\lvert\Delta\eta_{\ell\tau_{\text{had-vis}}}\rvert < 1.5$		$0.6 < \Delta R_{\tau_{\text{had-vis}}\tau_{\text{had-vis}}} < 2.5$ $\lvert\Delta\eta_{\tau_{\text{had-vis}}\tau_{\text{had-vis}}}\rvert < 1.5$
Coll. app. x_1/x_2	$0.1 < x_1 < 1.0$, $0.1 < x_2 < 1.0$	$0.1 < x_1 < 1.4$, $0.1 < x_2 < 1.2$		$0.1 < x_1 < 1.4$, $0.1 < x_2 < 1.4$

STXS measurements in $H \rightarrow \tau\tau$

NEW!

VBF inclusive	sub-leading jet $p_{\mathrm{T}} > 30\,\mathrm{GeV}$ $m_{jj} > 350\,\mathrm{GeV}$, $\lvert\Delta\eta_{jj}\rvert > 3$ $\eta(j_0) \times \eta(j_1) < 0$ lepton centrality: visible decay products of the τ leptons between VBF jets
VH inclusive	$60\,\mathrm{GeV} < m_{jj} < 120\,\mathrm{GeV}$ sub-leading jet $p_{\mathrm{T}} > 30\,\mathrm{GeV}$
$\mathbf{tt(0\ell)}\boldsymbol{H \rightarrow \tau_{\mathrm{had}}\tau_{\mathrm{had}}}$	# of jets ≥ 6 and # of b-jets ≥ 1 or # of jets ≥ 5 and # of b-jets ≥ 2
Boost inclusive	Not VBF inclusive Not VH inclusive $p_{\mathrm{T}}(H) > 100\,\mathrm{GeV}$

STXS measurements in $H \to \tau\tau$

NEW!

	Variable	VBF	ttH multiclass
Jet properties	Invariant mass of the two leading jets	•	
	$p_T(jj)$	•	
	Product of η of the two leading jets	•	
	Sub-leading jet p_T	•	
	η of the 5 leading jets		•
	Scalar sum of all jets p_T		•
	Scalar sum of all b-tagged jets p_T		•
	Best W-candidate dijet invariant mass		•
	Best t-quark-candidate three-jet invariant mass		•
Angular distances	$\Delta\phi$ between the two leading jets	•	
	$\Delta\eta$ between the two leading jets	•	
	Minimum ΔR between two jets		•
	Minimum ΔR between a b-tagged jet and a $\tau_{\text{had-vis}}$		•
	$\|\Delta\eta(\tau,\tau)\|$		•
	$\Delta R(\tau,\tau)$		•
τ prop.	$p_T(\tau\tau)$		•
	Sub-leading τ p_T		•
	Leading τ η		•
H cand. plus jets system	$p_T(Hjj)$	•	
$\vec{E}_T^{\text{miss}}$	Missing transverse momentum E_T^{miss}		•
	Smallest $\Delta\phi$ $(\tau, \vec{E}_T^{\text{miss}})$		•

STXS measurements in $H \rightarrow \tau\tau$

NEW!

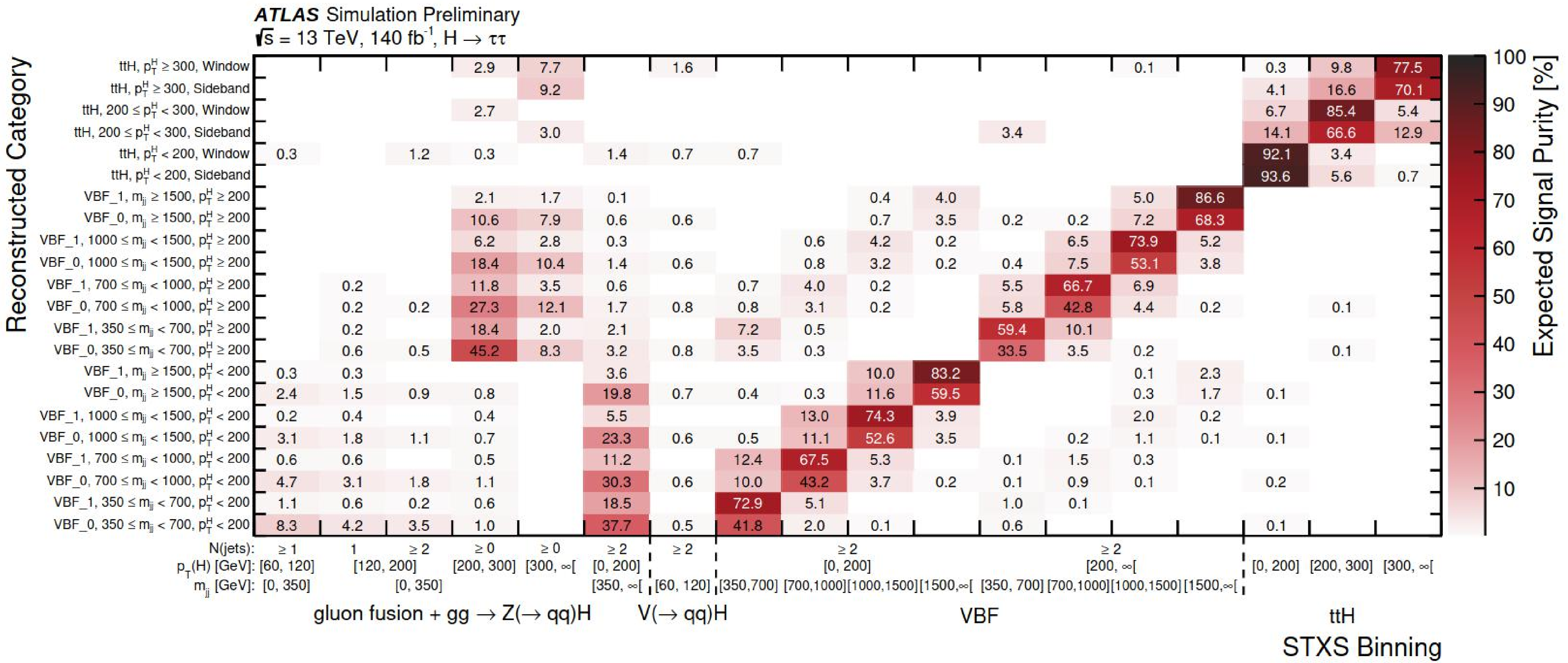

STXS measurements in $H \to \tau\tau$

- 18 POI fit corresponding to different STXS regions.
  - Better precision in VBF phase space for higher p_{T}^{H} and/or m_{jj} due to reduced SM backgrounds.
  - VBF cross-sections at lower m_{jj} and $p_{\mathrm{T}}^{H} < 200$ GeV slightly below SM predition.
  - Significant VBF-like ggH (ggH+2 jet production with mjj>350 GeV, pTH<200 GeV) contribution in reconstructed level categories targeting VBF signal.
    - → Anti-correlation in the measurements.

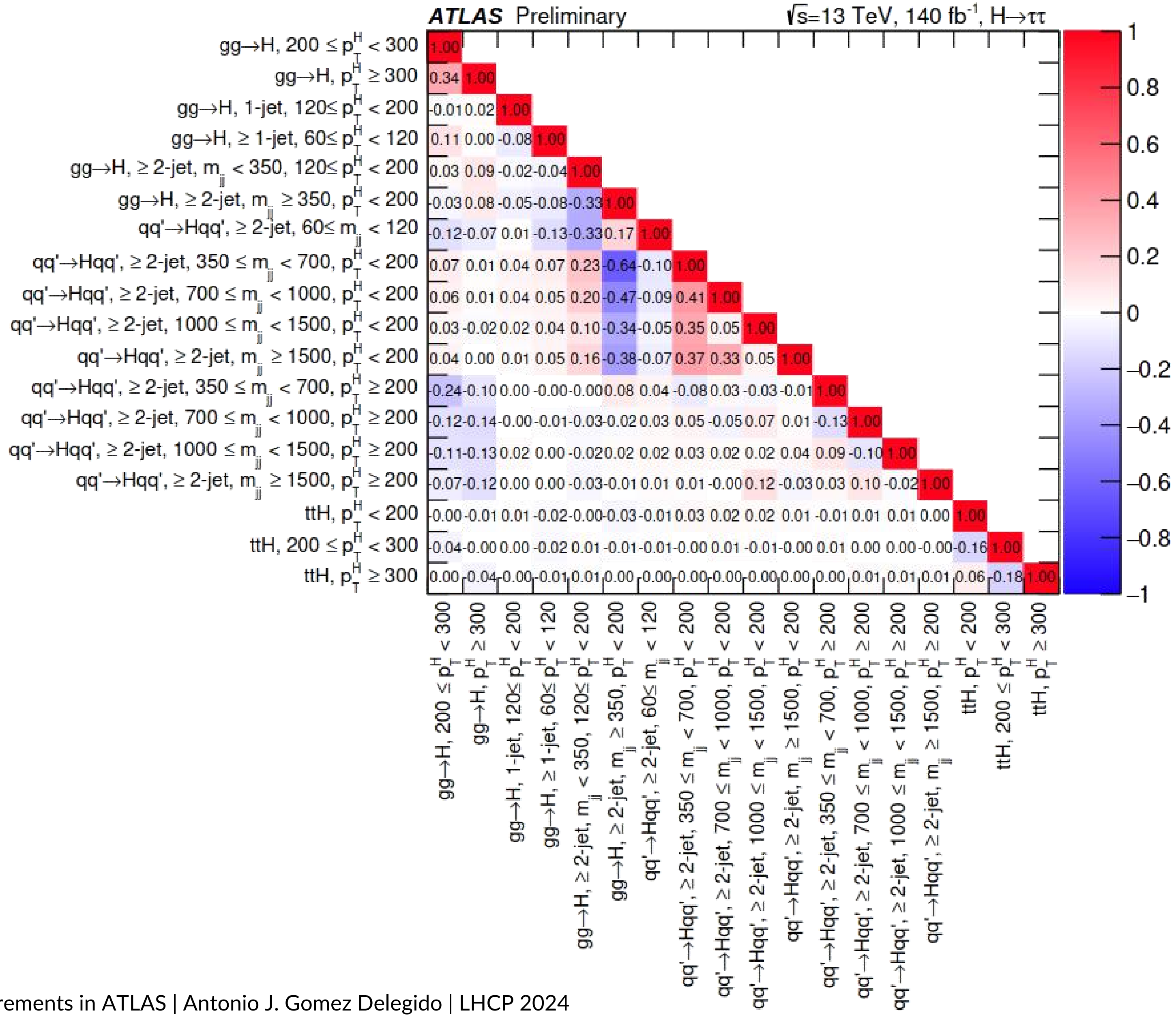

STXS measurements in $H \rightarrow \tau\tau$

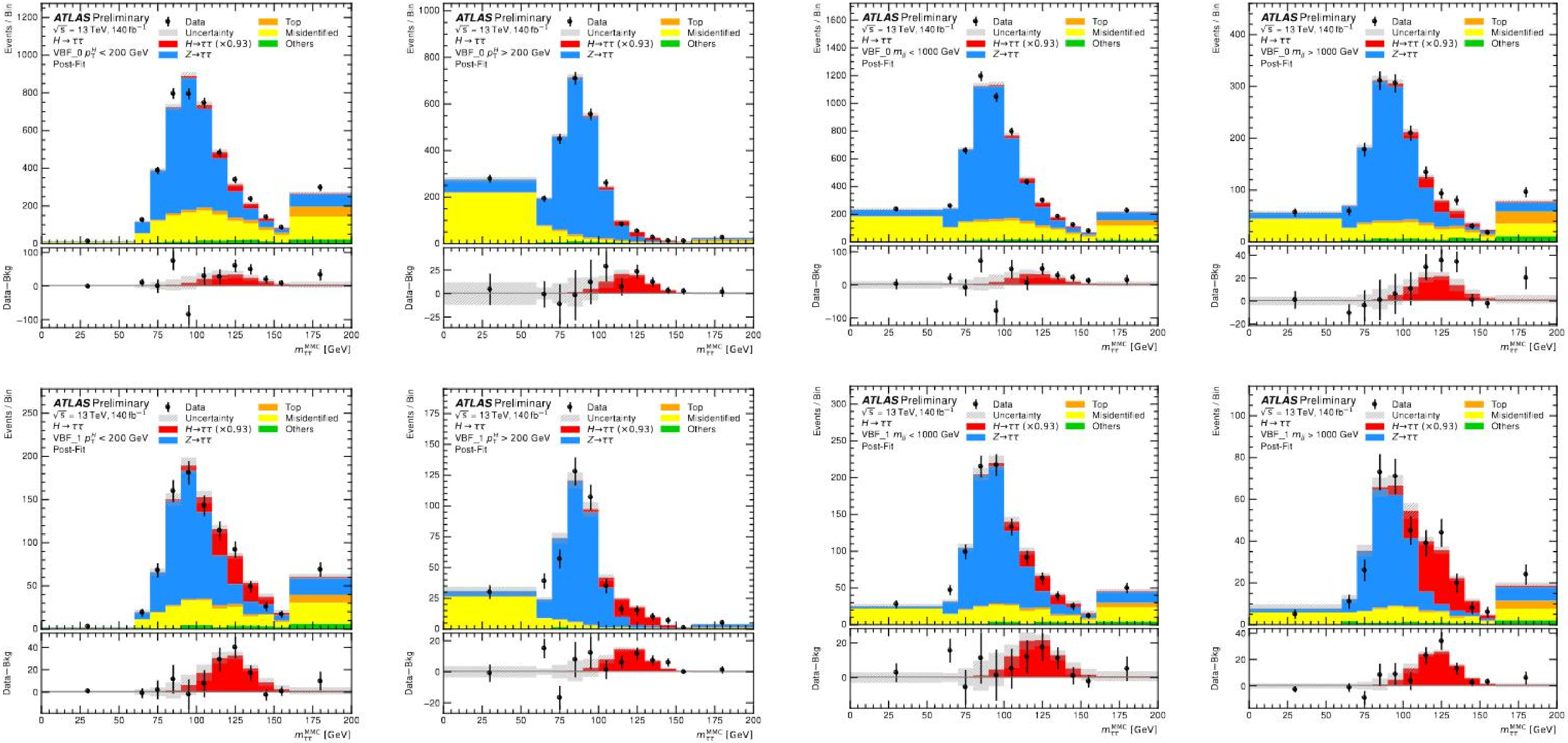

STXS measurements in $H \to \tau\tau$

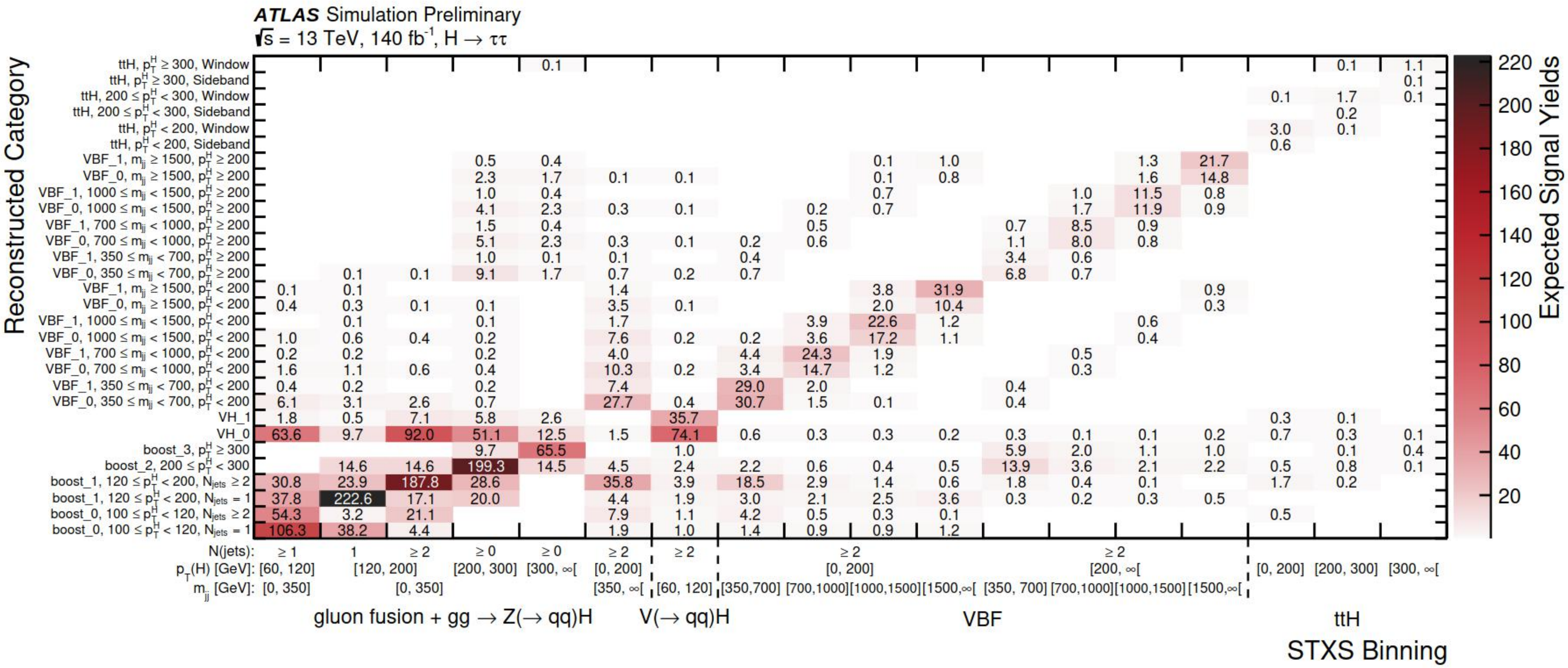

STXS measurements in $H \to \tau\tau$

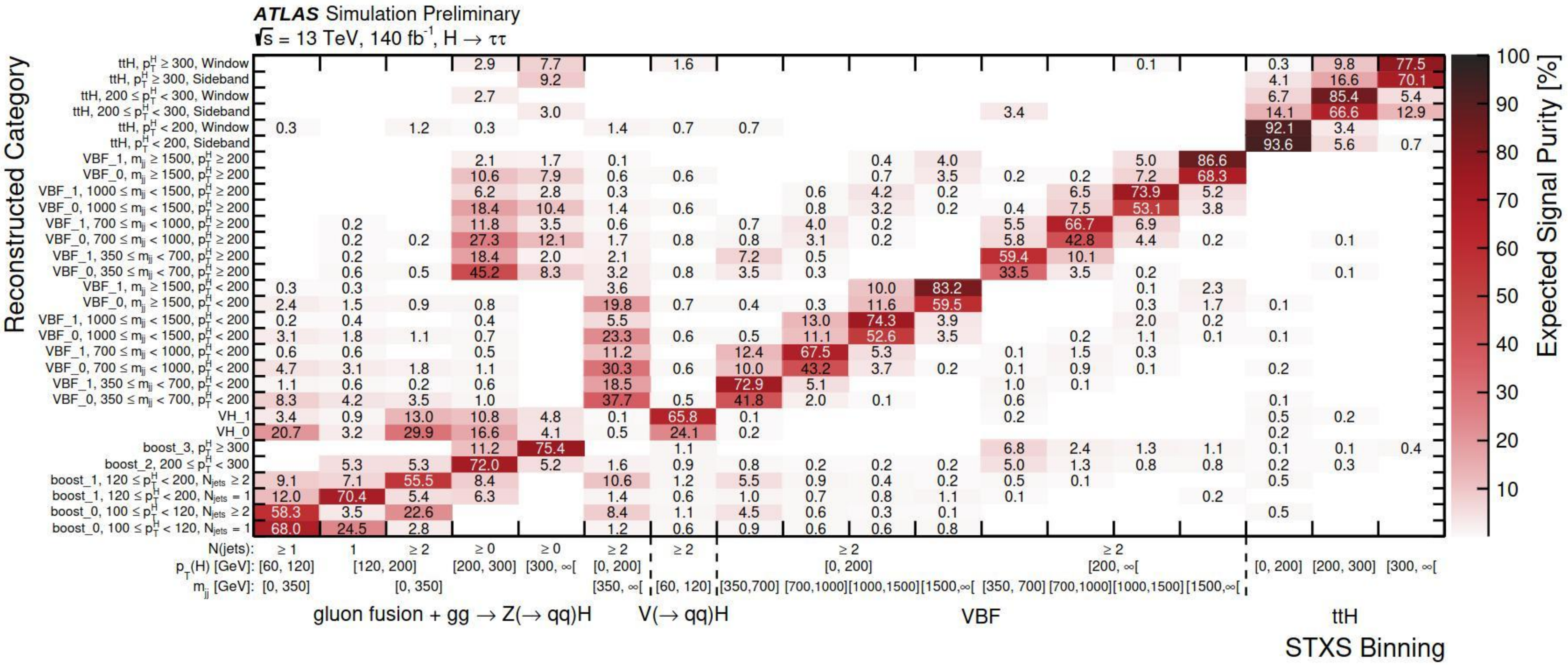

STXS measurements in $H \to \tau\tau$

NEW!

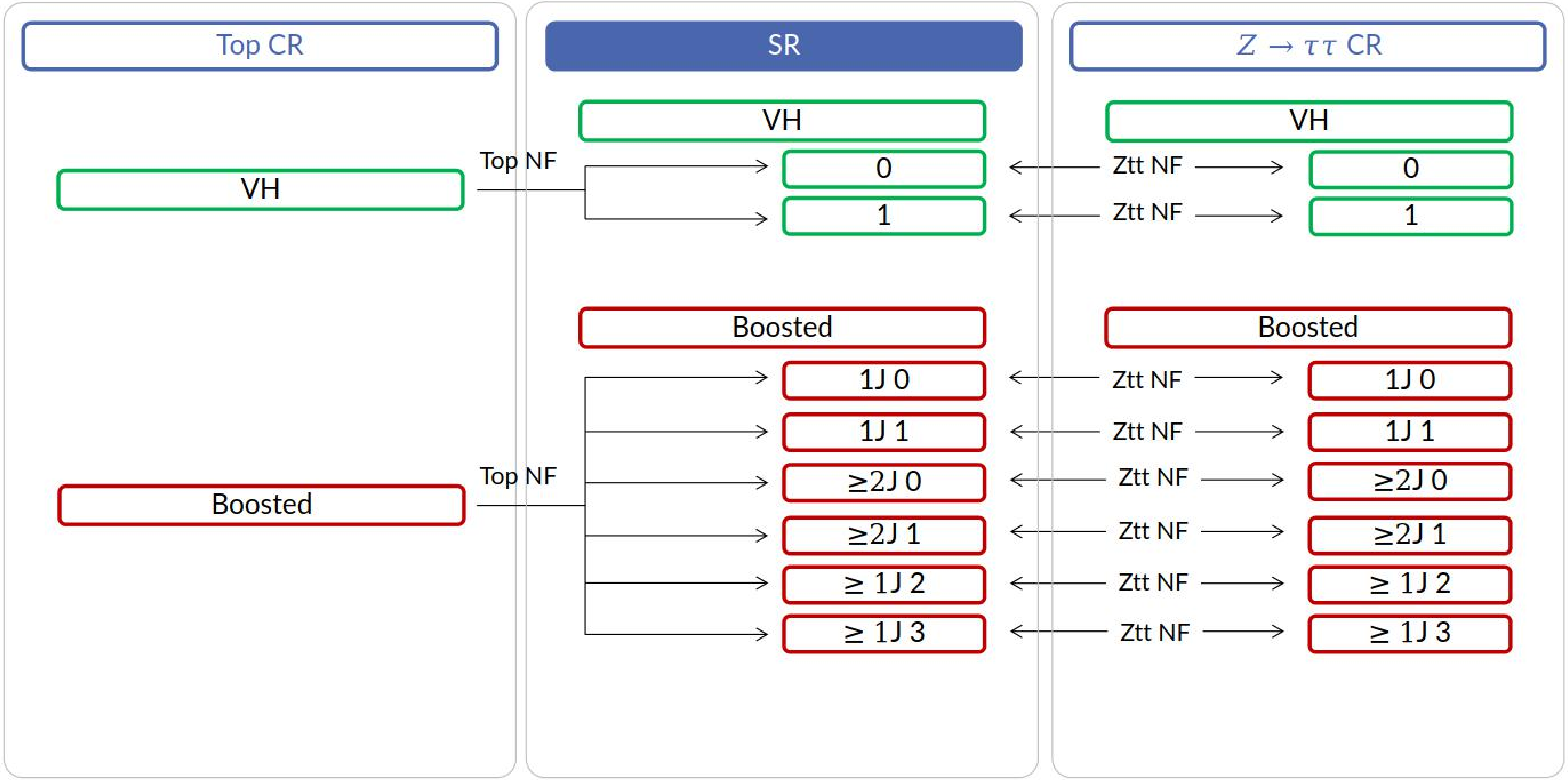

STXS measurements in $H \to \tau\tau$

NEW!

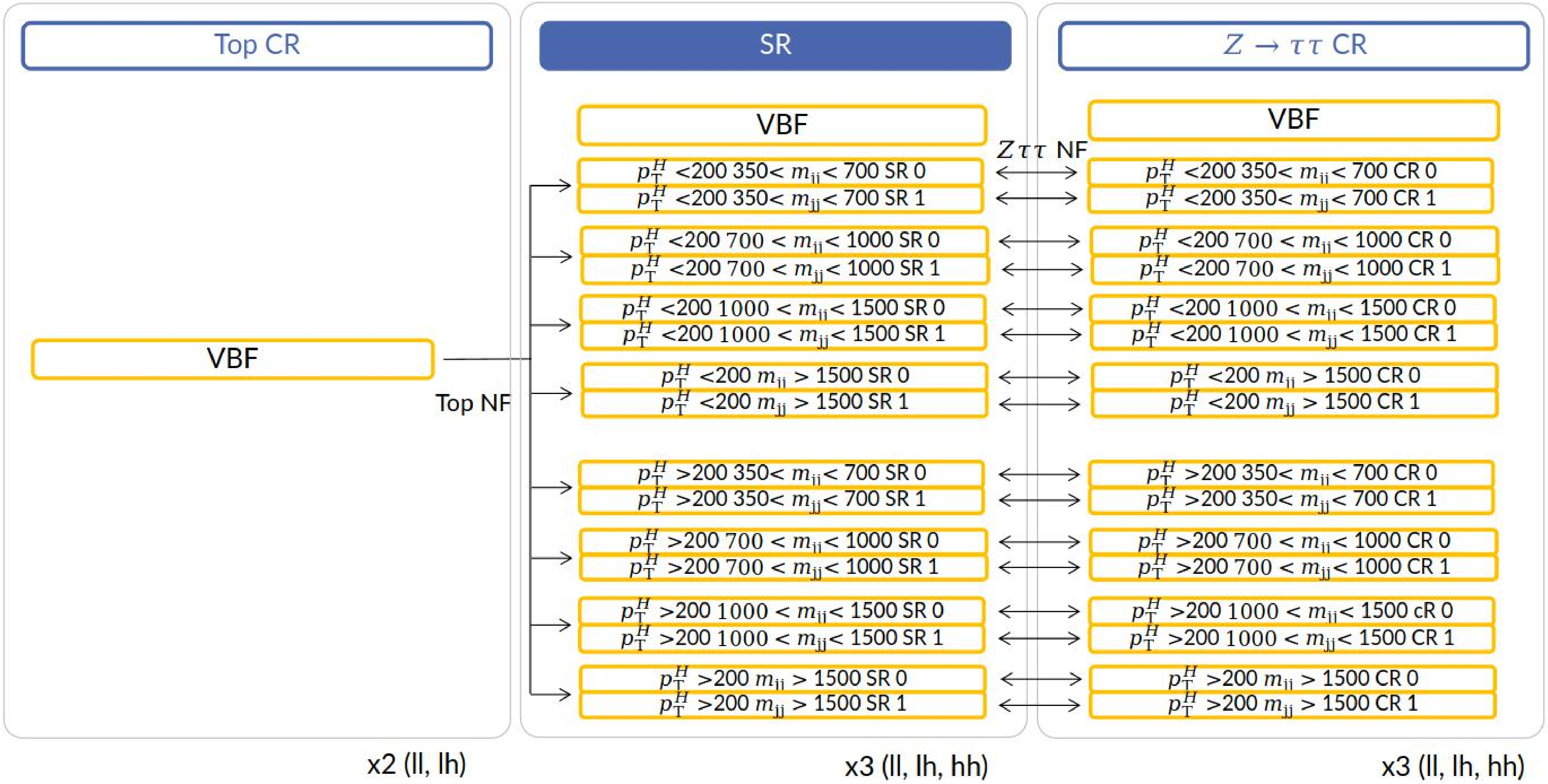

STXS measurements in $H \rightarrow \tau\tau$

NEW!

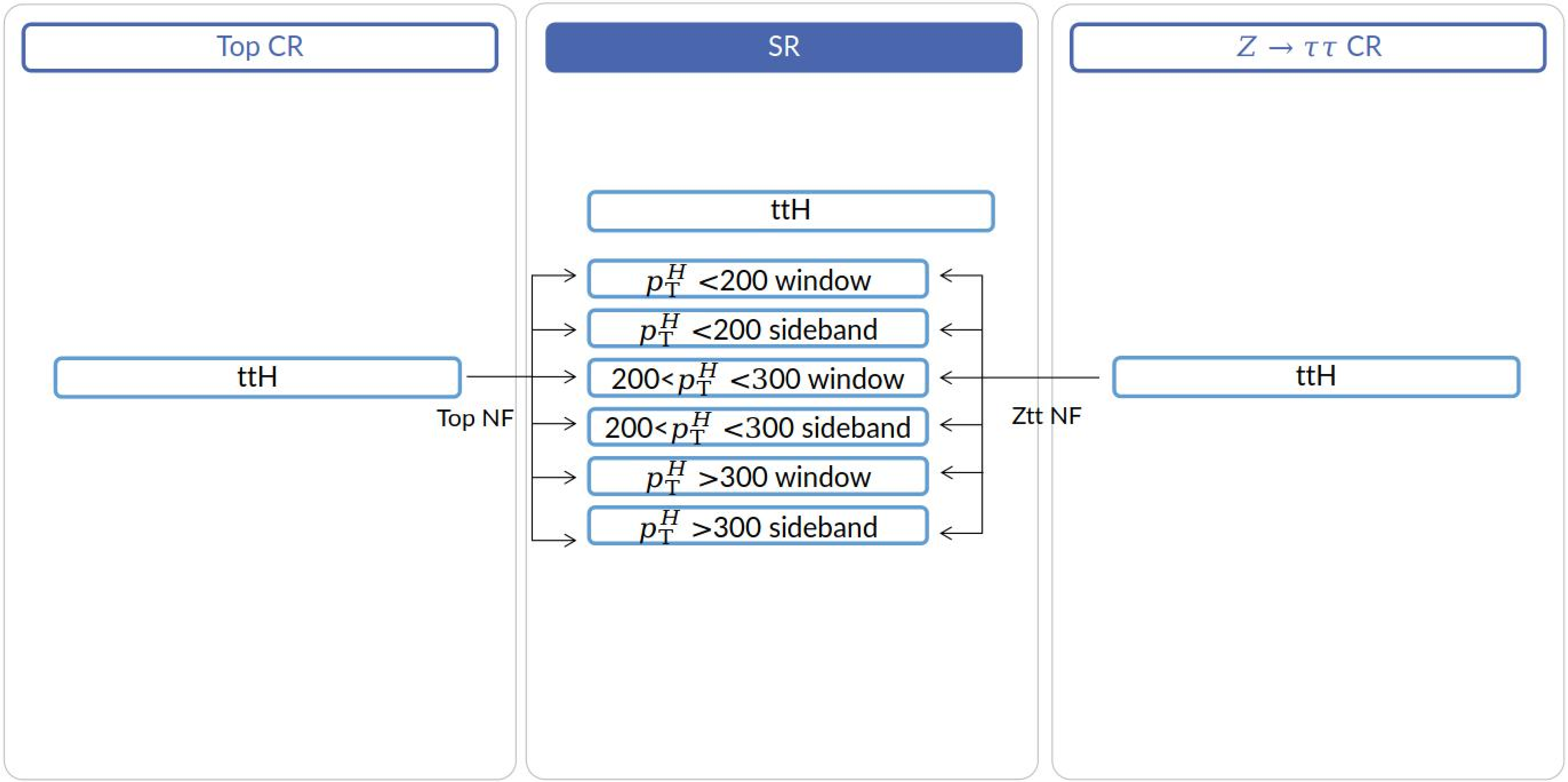

x1 (hh) x1 (hh) x1 (hh)

Searches for rare Higgs boson decays

Phys. Lett. B 812 (2021) 135980

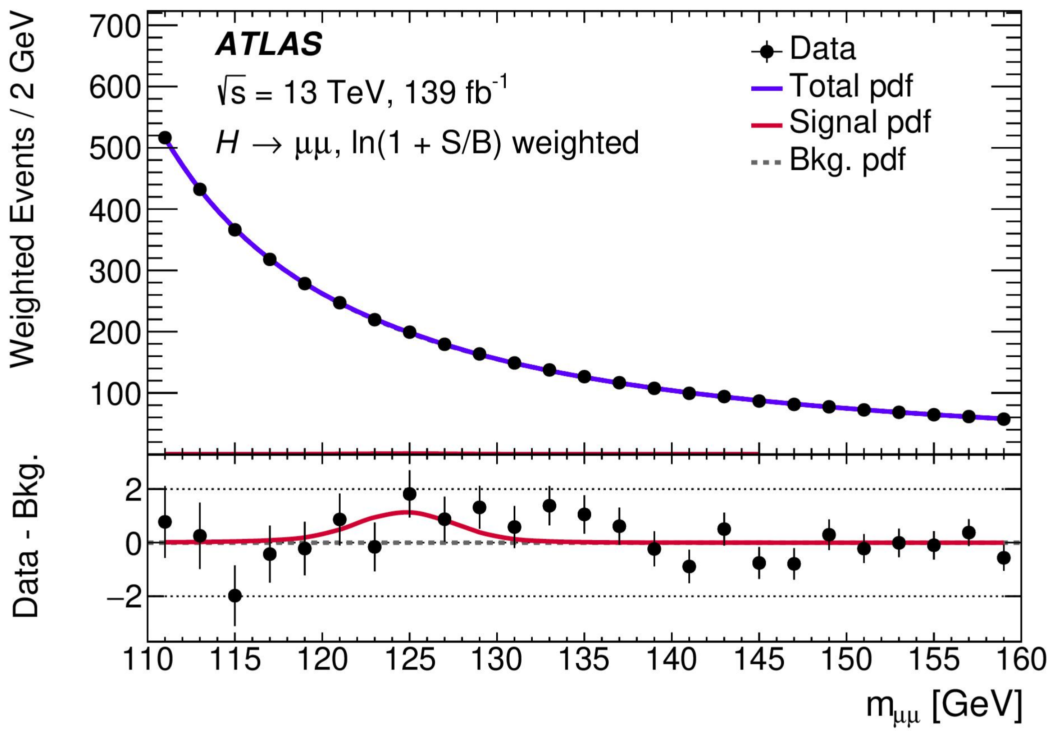

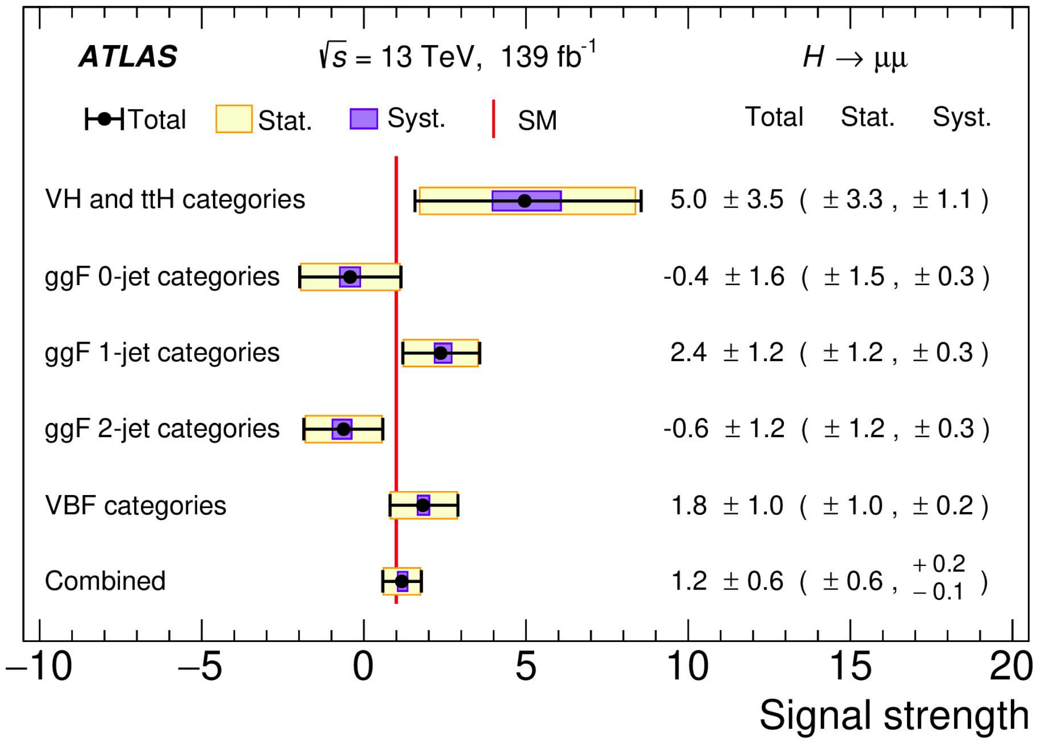

Searches for rare Higgs boson decays

Eur. Phys. J. C 82 (2022) 717

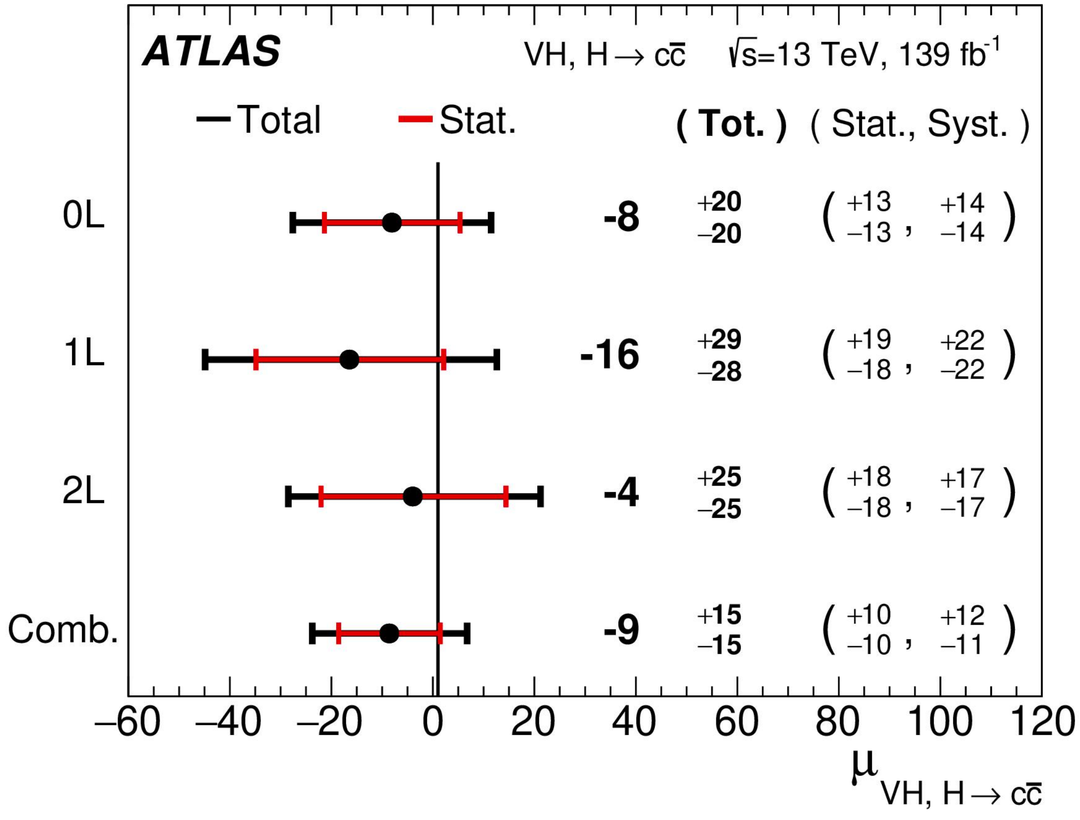

Source of uncertainty		$\mu_{VH(c\bar{c})}$	$\mu_{VW(cq)}$	$\mu_{VZ(c\bar{c})}$
Total		15.3	0.24	0.48
Statistical		10.0	0.11	0.32
Systematic		11.5	0.21	0.36
Statistical uncertainties				
Signal normalisation		7.8	0.05	0.23
Other normalisations		5.1	0.09	0.22
Theoretical and modelling uncertainties				
$VH(\to c\bar{c})$		2.1	< 0.01	0.01
$Z+$jets		7.0	0.05	0.17
Top quark		3.9	0.13	0.09
$W+$jets		3.0	0.05	0.11
Diboson		1.0	0.09	0.12
$VH(\to b\bar{b})$		0.8	< 0.01	0.01
Multi-jet		1.0	0.03	0.02
Simulation samples size		4.2	0.09	0.13
Experimental uncertainties				
Jets		2.8	0.06	0.13
Leptons		0.5	0.01	0.01
E_T^{miss}		0.2	0.01	0.01
Pile-up and luminosity		0.3	0.01	0.01
Flavour tagging	c-jets	1.6	0.05	0.16
	b-jets	1.1	0.01	0.03
	light-jets	0.4	0.01	0.06
	τ-jets	0.3	0.01	0.04
Truth-flavour tagging	ΔR correction	3.3	0.03	0.10
	Residual non-closure	1.7	0.03	0.10